Physics of and Achievements with the H-mode

F. Wagner
Max-Planck Institut für Plasmaphysik
EURATOM Association
Greifswald

Goal of fusion: energy source from fusion reaction

Conditions to be met: Lawson-conditions;
triple product: $n_i T_i \tau_E > 5\ 10^{21}\ m^{-3}keVs$

0-dim energy balance:

$$\dot{W} = P - \frac{W}{\tau_E}$$

Steady-state: $$\tau_E = \frac{W}{P}$$

Power switch-off: $$\dot{W} = -\frac{W}{\tau_E}$$

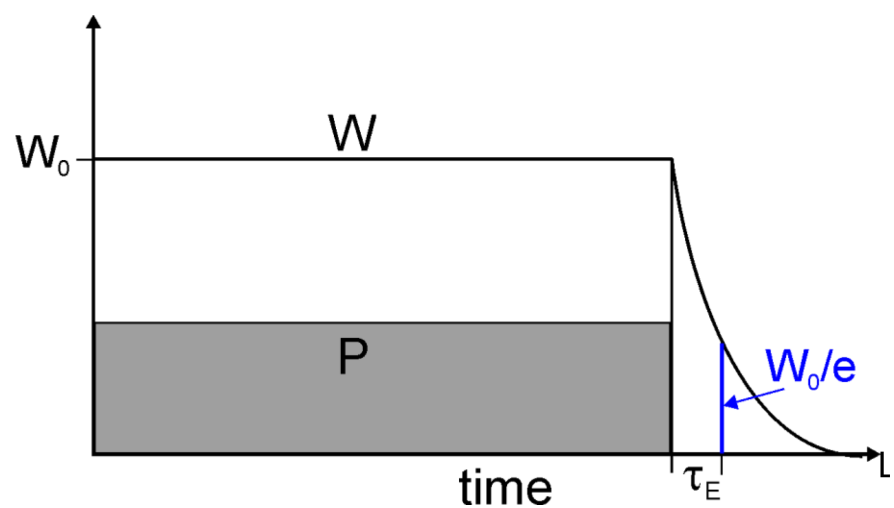

Physics of and Achievements with the H-mode

F. Wagner
Max-Planck Institut für Plasmaphysik
EURATOM Association
Greifswald

Goal of fusion: energy source from fusion reaction

Conditions to be met: Lawson-conditions;
triple product: $n_i T_i \tau_E > 5\ 10^{21}\ m^{-3}keVs$

0-dim energy balance:

$$\dot{W} = P - \frac{W}{\tau_E}$$

Steady-state: $$\tau_E = \frac{W}{P}$$

Power switch-off: $$\dot{W} = -\frac{W}{\tau_E}$$

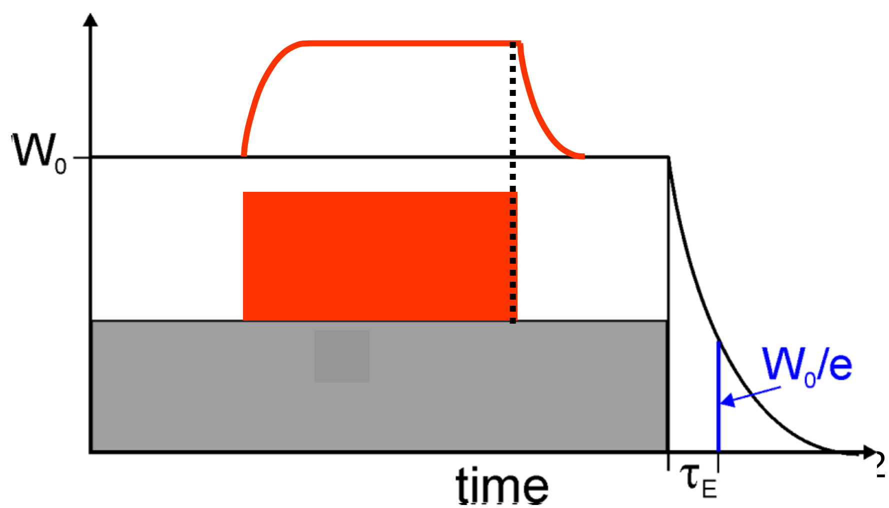

F. Wagner
Max-Planck Institut für Plasmaphysik
EURATOM Association
Greifswald

Goal of fusion: energy source from fusion reaction

Conditions to be met: Lawson-conditions;
triple product: $n_i T_i \tau_E > 5\ 10^{21}\ m^{-3}keVs$

0-dim energy balance:

$$\dot{W} = P - \frac{W}{\tau_E}$$

Steady-state: $$\tau_E = \frac{W}{P}$$

Power switch-off: $$\dot{W} = -\frac{W}{\tau_E}$$

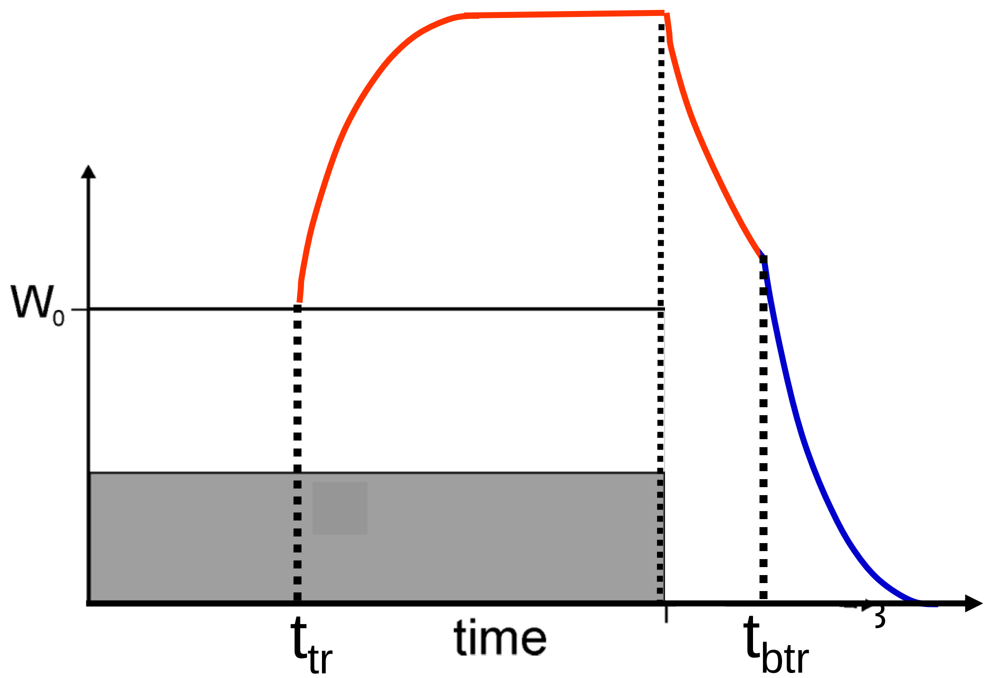

1 Confinement and transport

Thermal plasma energy content: $$W = 2 \times \frac{3}{2} \int nT \mathrm{d}^3 r \approx 3V\bar{n}\bar{T}$$

Power flux across edge in steady-state: $$P = 2 \times Sn\chi \nabla T|_{\mathrm{edge}} \approx 2Sn\bar{\chi}\frac{\bar{T}}{a}$$

Confinement and diffusivity: $$\tau_E \approx \frac{3a^2}{4\bar{\chi}}$$

$\chi \sim 1 m^2/s$;
$a \sim 1 m$;
$\tau_E \sim 1 s$

Importance of τ_E:

Triple product: $nT\tau_E \sim \tau_E^2$

Fusion power: $P_{fus} \sim \beta^2 B^4 \sim \tau_E^2$

Transport in toroidal systems

Random walk conception: $D \sim \Delta x^2/\Delta t$

Parallel to magnetic field: $\Delta x \sim \lambda$; $\Delta t \sim \tau_{coulomb}$

Perpendicular to magnetic field: $\Delta x \sim \rho_L$; $\Delta t \sim \tau_{coulomb}$

In toroidal geometry: $\Delta x \sim$ banana width; $\Delta t \sim \tau_{trapped\text{-}free}$;
fraction of trapped particles enters

In helical systems (3D): helical ripple enters; collisionless losses

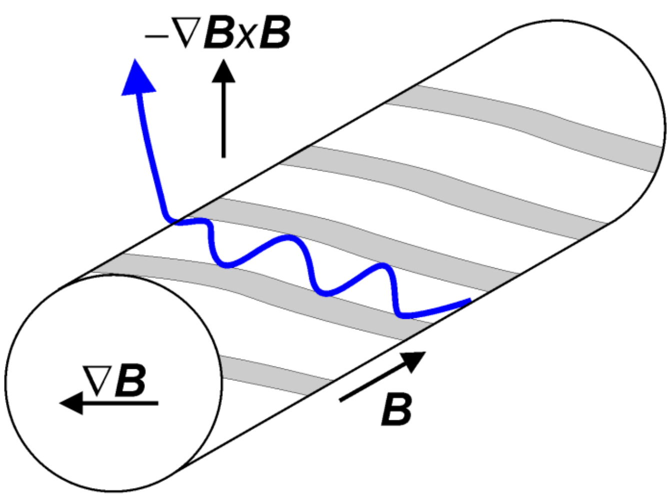

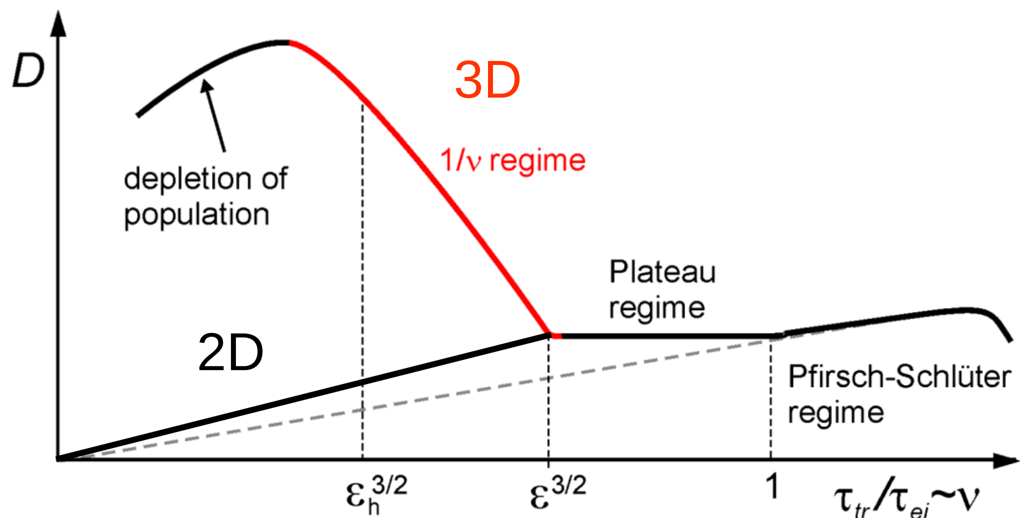

=> Stellarator optimisation by quasi-symmerty

Turbulent transport

microinstabilities drive turbulent eddies:

radial extent (radial correlation lenght ρ_c) ~ 1 - 2 cm

typical lifetime of turbulent eddies (correlation time τ_c): 0.5 - 1 ms

$\Rightarrow$ - convective transport

- heat flux $q = n \langle\tilde{T}\tilde{v}\rangle$ & particle flux $\Gamma = \langle\tilde{n}\,\tilde{v}\rangle$
- effective transport coefficients

$$D \sim \rho_c^2/\tau_c = \gamma\, k_\perp^{-2} \sim 1\ \mathrm{m}^2/\mathrm{s}$$

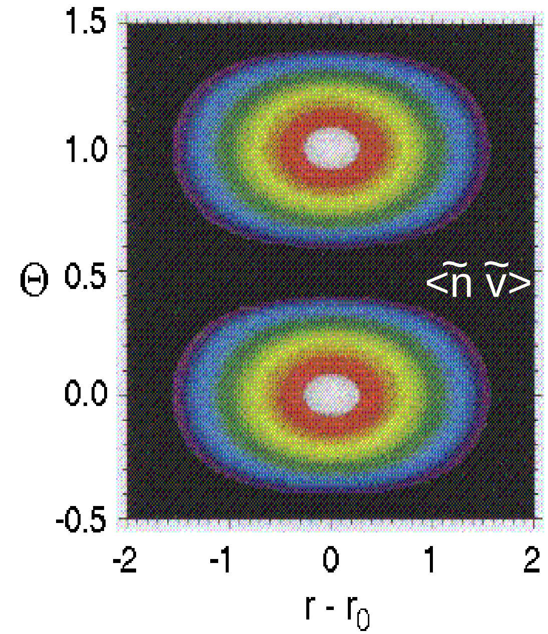

Potential

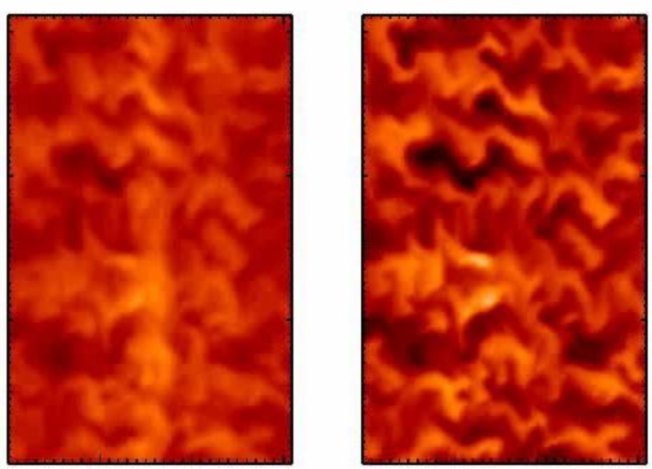

Density

poloidal

∇p

$\otimes\ \boldsymbol{B}$

radial

Scaling Laws

- **Regression analysis** with the ansatz

$$\tau_E = 10^{\alpha_x} a^{\alpha_a} R^{\alpha_R} P^{\alpha_P} \bar{n}_e^{\alpha_n} B^{\alpha_B} \iota_{2/3}^{\alpha_\iota}$$

Tokamak scaling
L-mode scaling (1989)
H-mode scaling (H(y,2))

Stellarator scaling
ISS95, ISS04

- **ISS95** for stellarators (and tokamaks)
  - minor radius $\alpha_a = +2.21$
  - major radius $\alpha_R = +0.65$
  - heating power $\alpha_P = -0.59$
  - density $\alpha_n = +0.51$
  - magnetic field $\alpha_B = +0.84$
  - Iota $\alpha_\iota = +0.40$

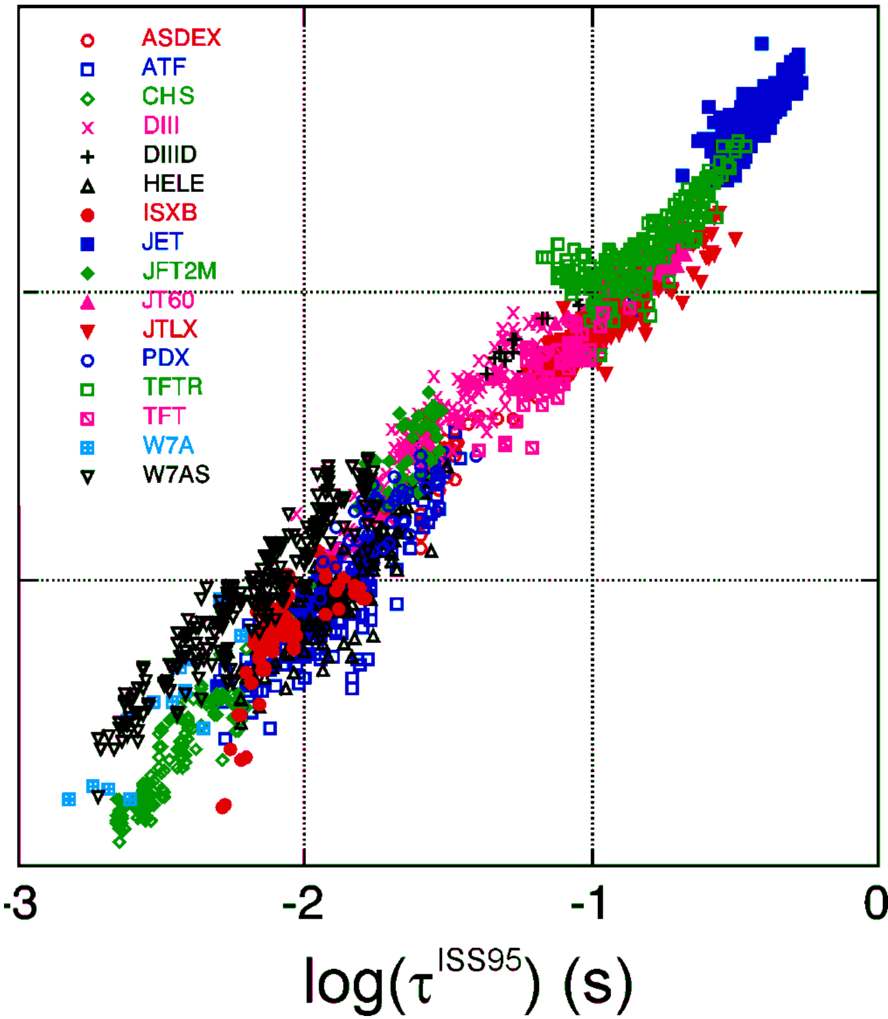

Similar confinement times in tokamaks and stellarators

Importance of improved confinement

$Q = P_{fus}/P_{ext}$

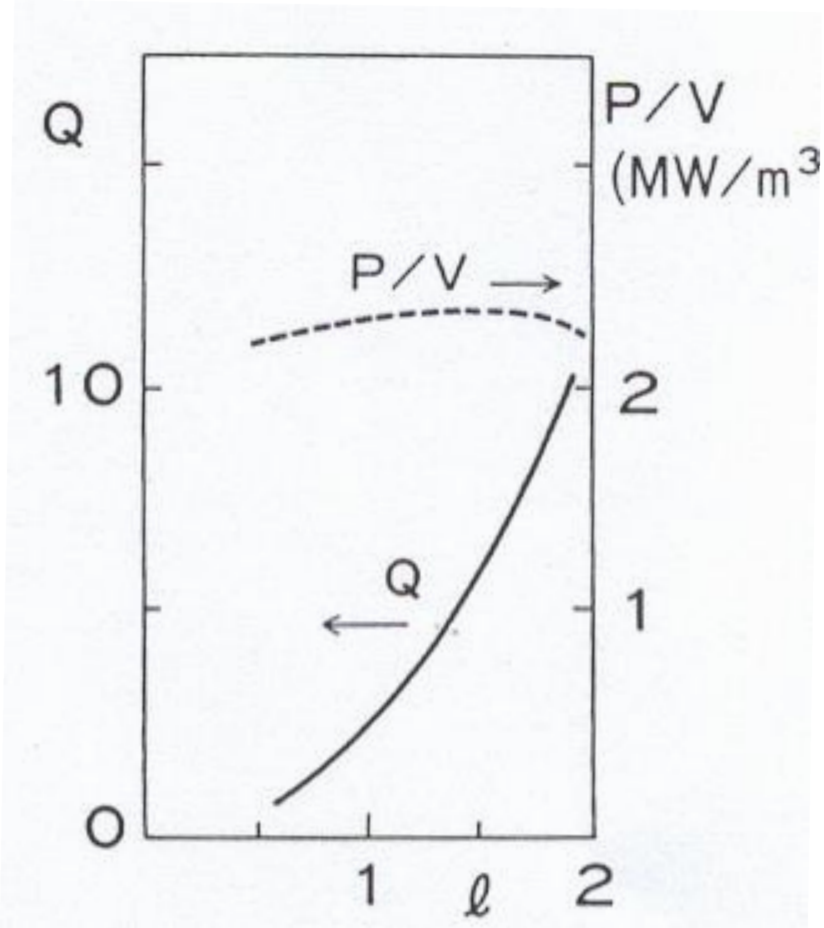

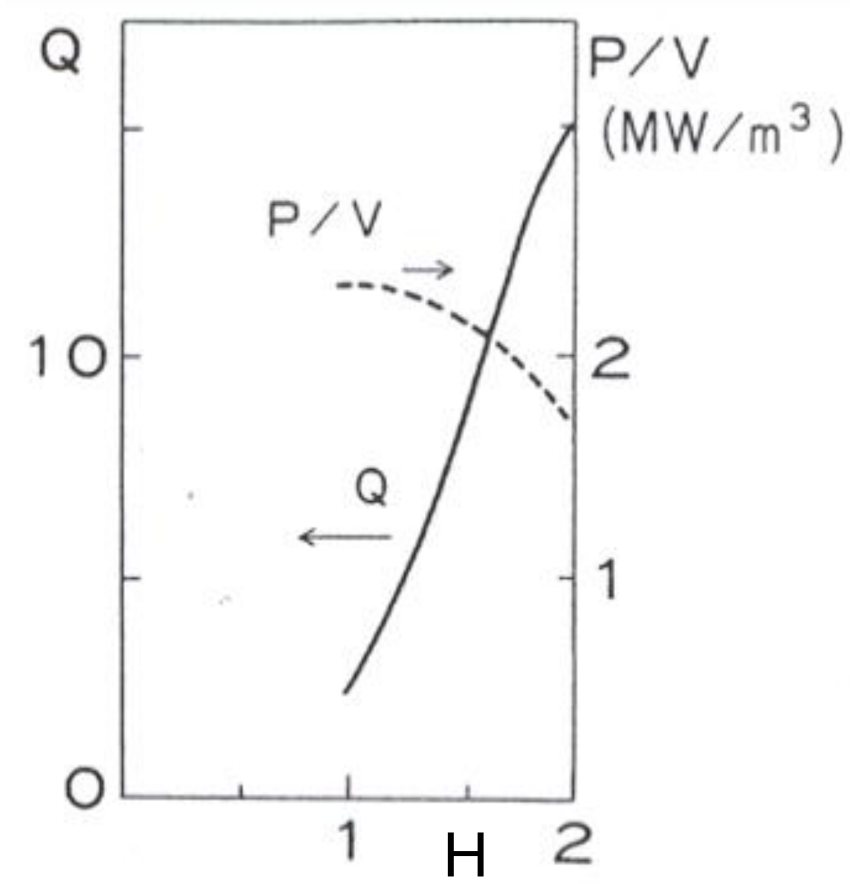

K.Itoh et al.

Characteristics of the H-mode transition

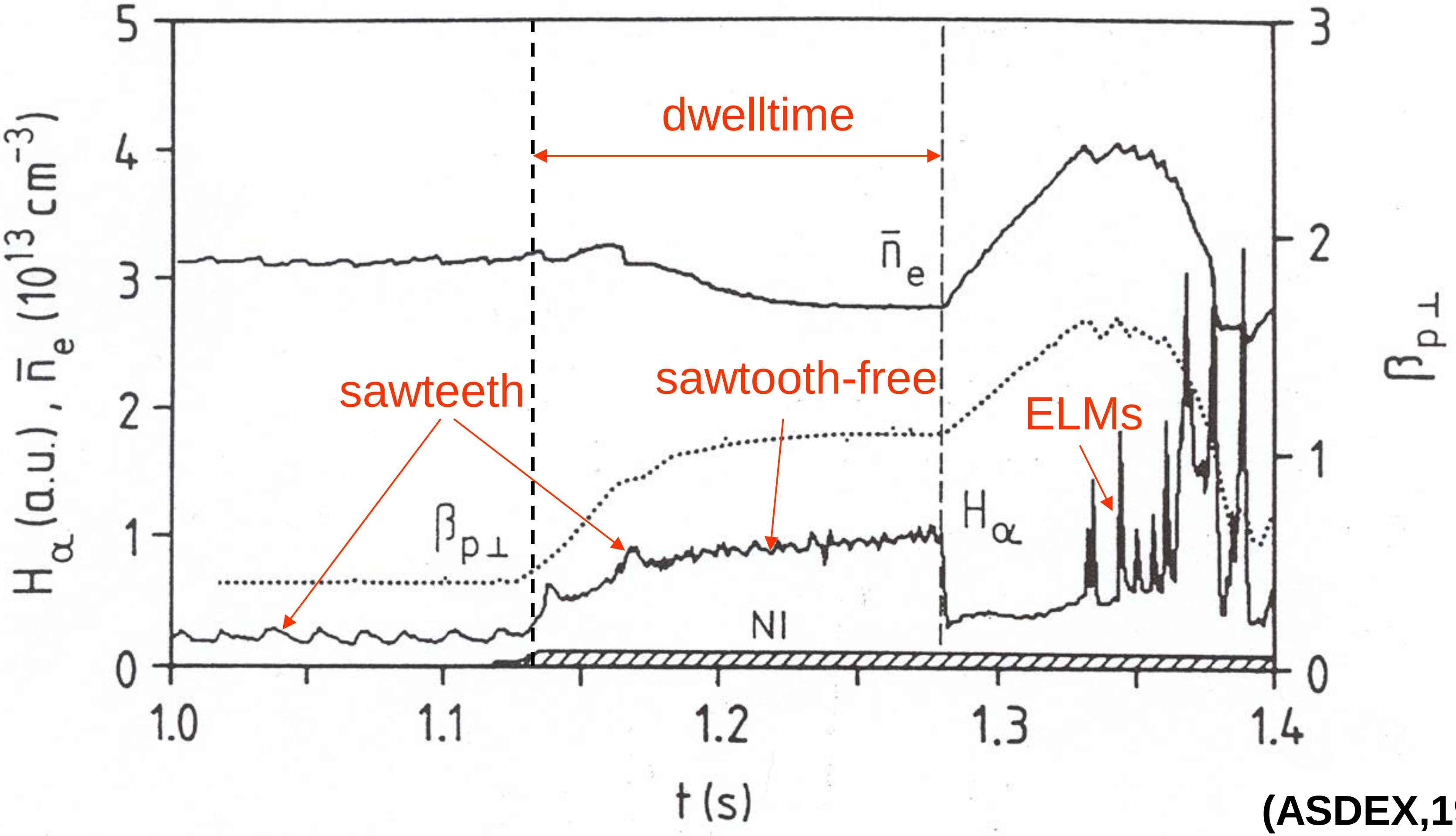

(ASDEX,1982)

The main features of the H-mode

the marker for the transition is the drop in the H_α-radiation
a spontaneous and distinct transition out of state in transport equilibrium
both energy- and particle confinement time increase simultaneously
new instabilities appear in the H-phase: ELMs, edge-localised modes

The plasma edge becomes quiescent and sharp

NSTX

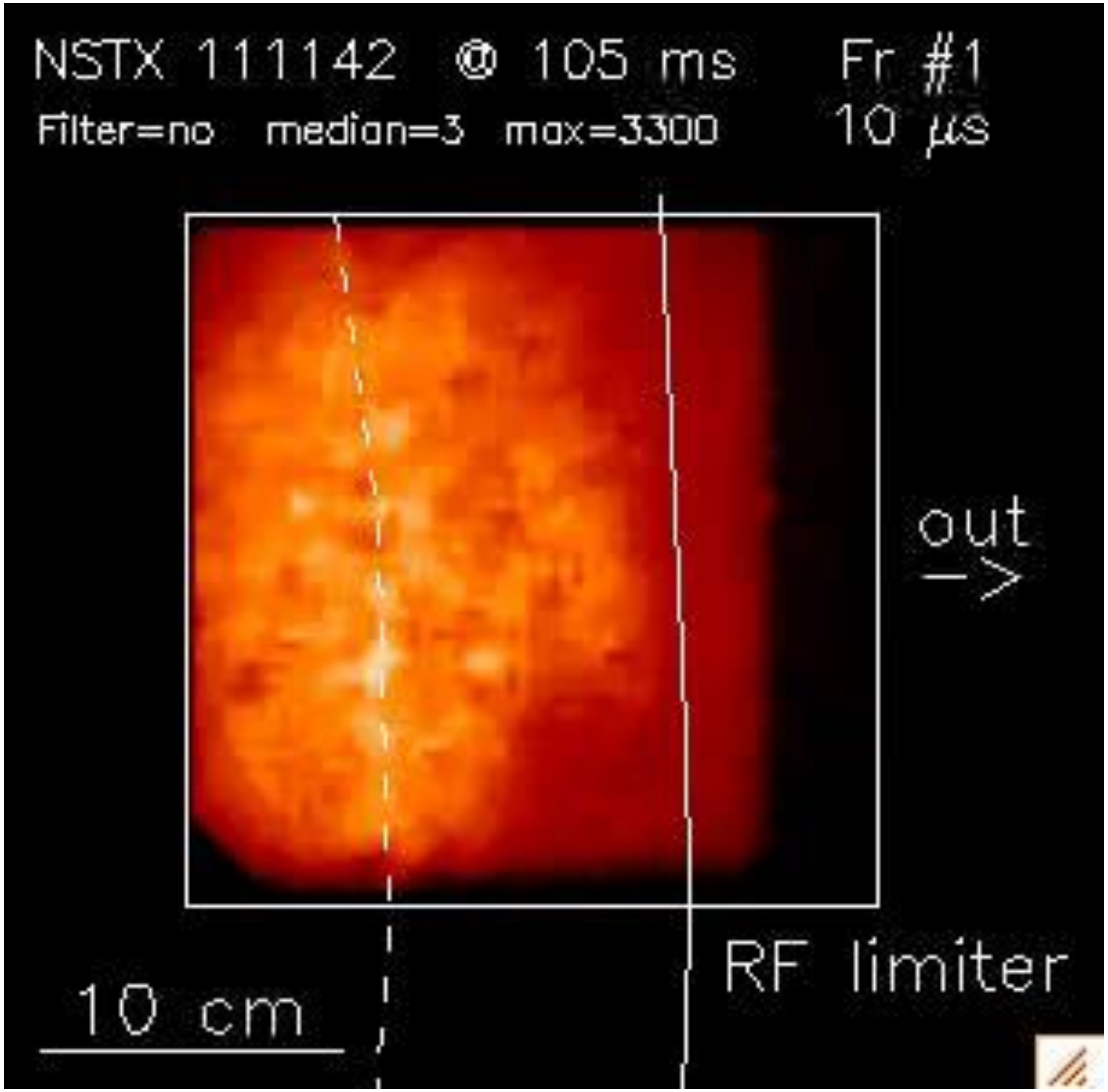

Different edge activities in L- and H-modes

Turbulent edge filaments in L-mode and in H-mode between ELMs

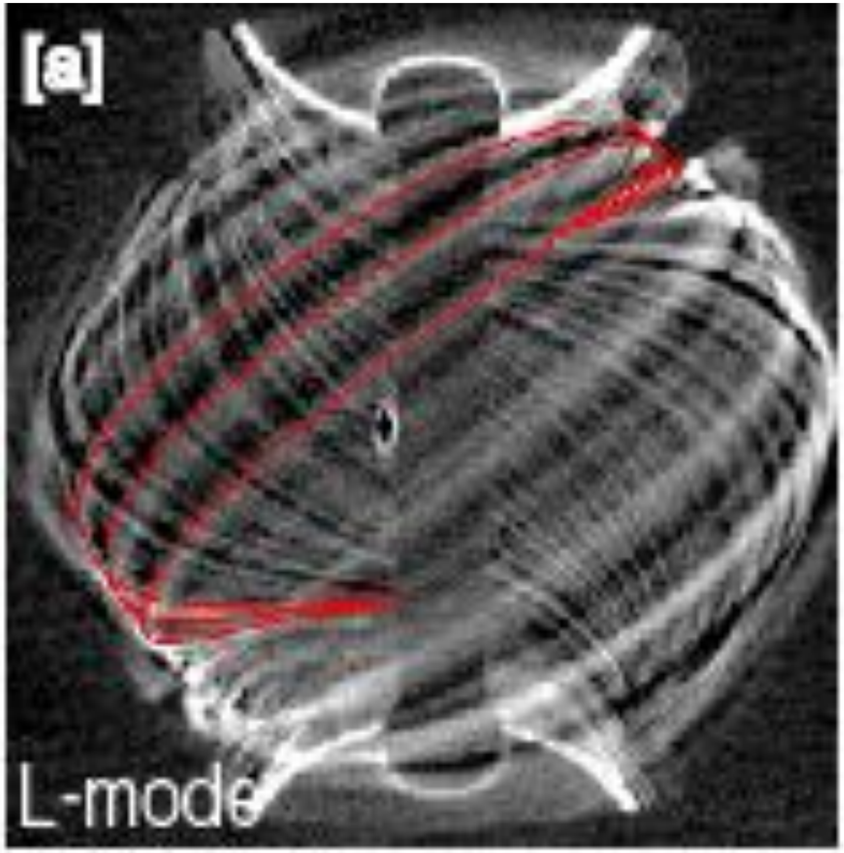

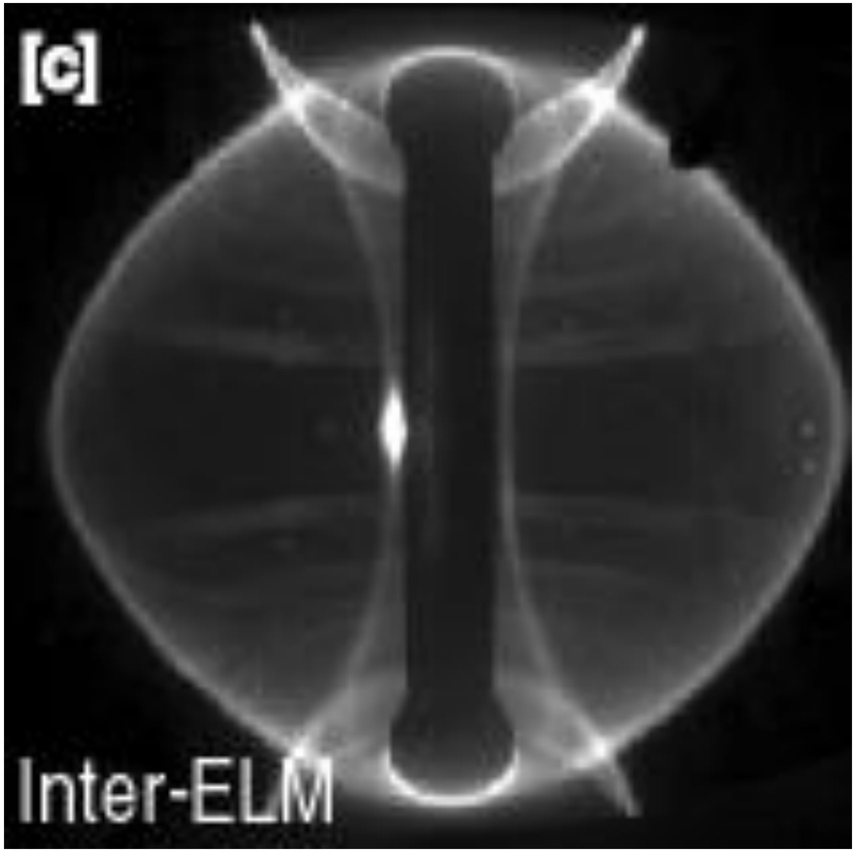

N. Ben Ayed, MAST

2 Initial observations

(1) L- and H-modes differ in energy confinement time by about a factor of two:
two operational branches exist; the space in between in not accessible.
energy, particle, impurity, and momentum confinement improve simultaneously

(2) The H-mode transition has a power threshold P_{th}:
Obviously, a critical condition has to be met via heating.

(3) There is a dwell time after the heating power has been increased
A formation process has been initiated by stepping up the heating power with a time scale depending also on external settings (power, configuration (SN^+, DN, SN^-)).

(4) When the heating power has been switched off, the plasma remains in the H-phase again for a dwell time in the order of the confinement time:
The plasma does not hover at the transition condition but goes deeper into the H-mode domain. The dwell-time points to the existence of an hysteresis.
The back-transition is of specific interest because the plasma is not driven but evolves in equilibria according to its internal time scales. Also the back transition occurs in a distinct step – the gap between H- and L-mode branches.

(5) There is also a low density threshold:
the critical transition condition cannot be met
(local circumstances: radiation, locked modes**).**

Initial observations

(6) Large sawteeth can trigger the H-mode:

The critical parameter seems to be a local condition at the plasma edge, which can be met by a thermal wave

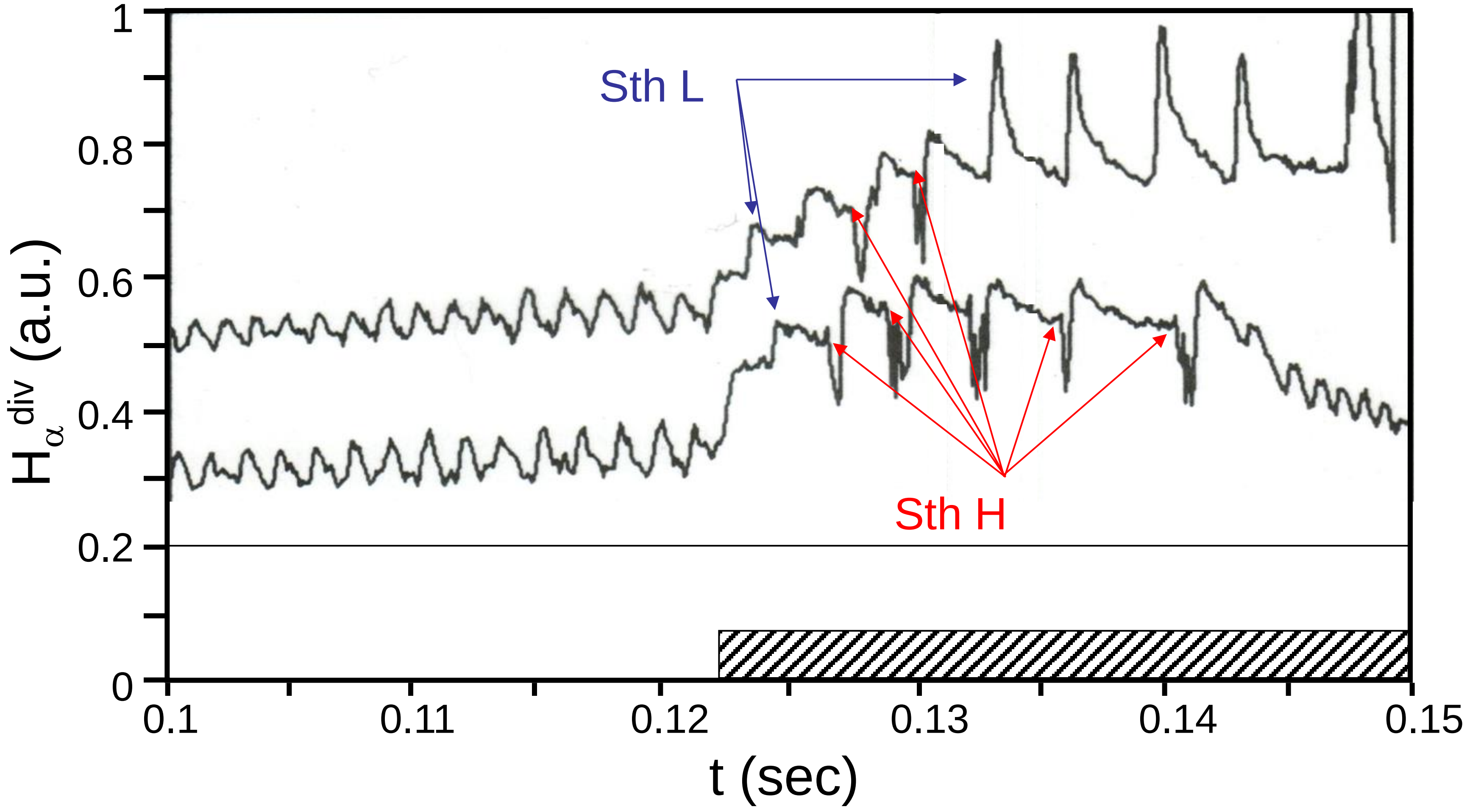

(7) ELMs appeared in the H-mode as a new type of edge instability.

Overview over transition characteristics

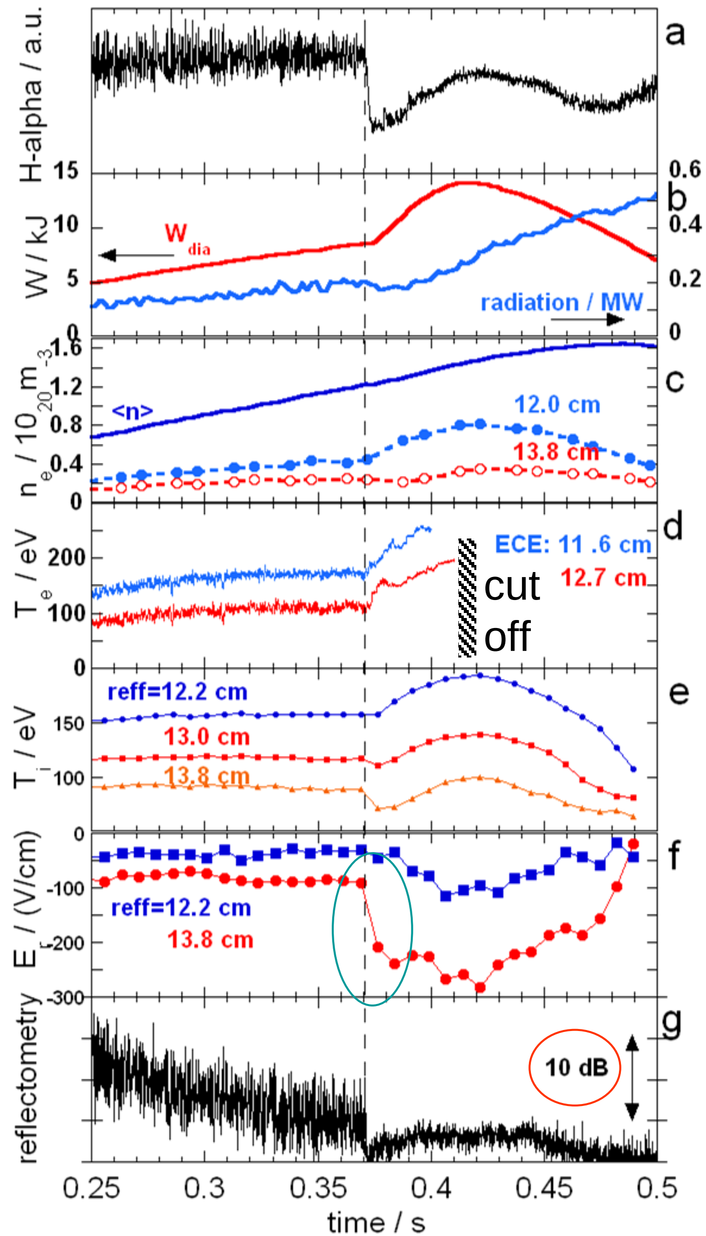

Major results from W7-AS

Implication of the stellarator H-mode:

-H-mode is a ubiquitous characteristics of toroidal confinement

- iota at the separatrix is finite: the magnetic shear anomaly of the divertor configuration is not essential

-the ambipolarity is determined by $\Gamma_e = \Gamma_i$ (enforced ambipolarity)

-toroidal rotation is highly damped

-P_{th} like τ_E do not show an isotopic effect

Relevant differences to tokamaks

-$P_{th}^{stell} < P_{th}^{tok}$ (by ~ factor 2)

-H-mode in selected iota-windows only

Dependencies of the power threshold

P_{th} is lower

(1) with separatrix instead of limiter operation

(2) in deuterium instead of hydrogen plasmas

(3) in clean instead of dirty plasmas

(4) with gas fuelling from the divertor or the high-field side instead of the low-field side

(5) in single null plasmas with the ion-grad B-drift to the X-point (SN^+) instead of away from it (SN^-) ;
in double null plasmas (DN), P_{th} is in between:

Obviously, a supporting / prohibiting aspect nullifies in the symmetric case.

Specific observations

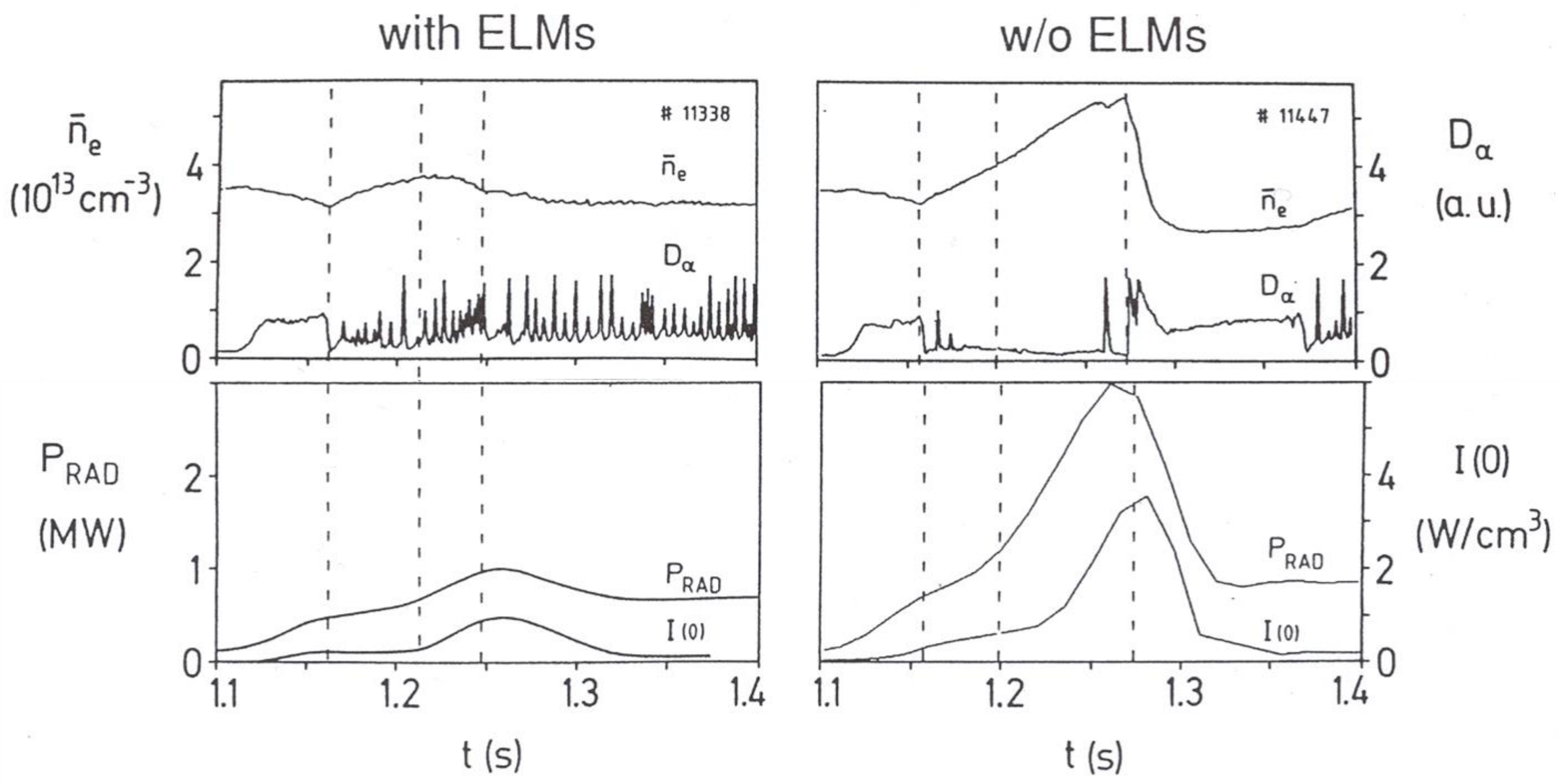

Two variants of the H-mode: with and without ELMs

with ELMs: moderate increase in confinement time
suitable for steady-state operation

without ELMs: transiently better confinement; impurity accumulation

Change in the prominent mode activity

Post-beam-pulse (PBP) T_e-rise

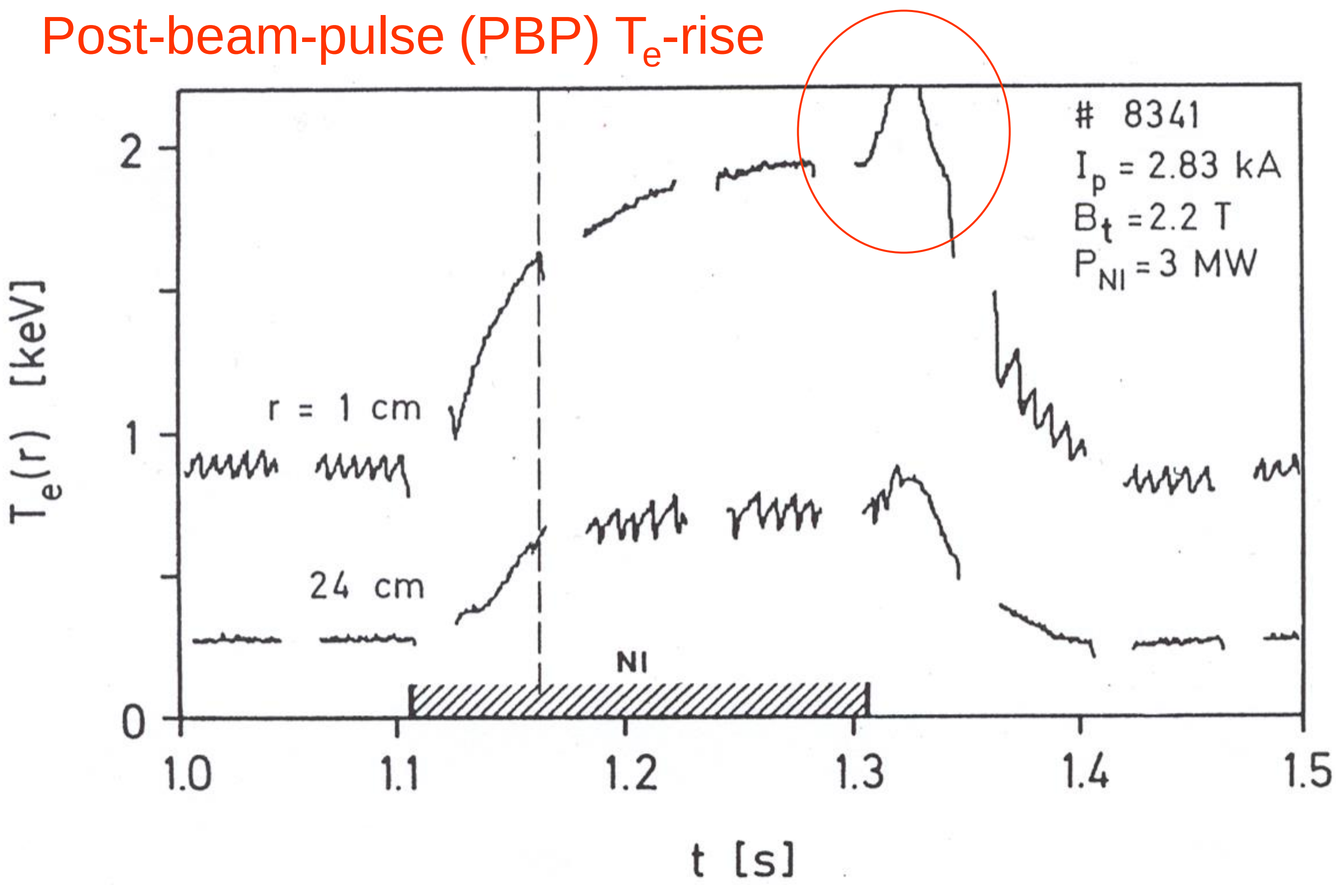

Relaxations in the plasma core during ohmic heating: Sawteeth

Relaxations at the plasma edge in the H-phase: ELMs

Initial and final dwell times

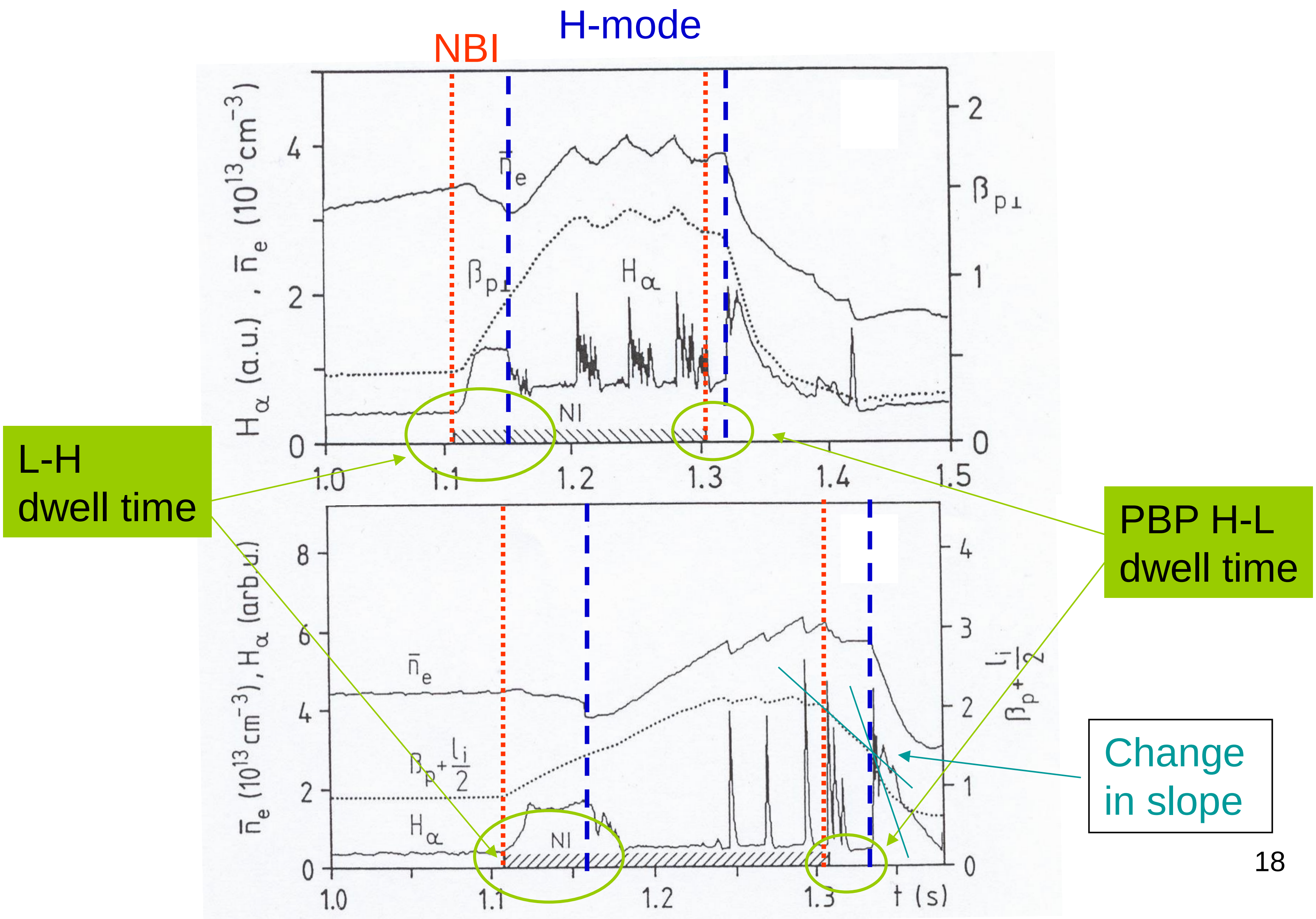

Short H-phases in the PBP T_e-rise

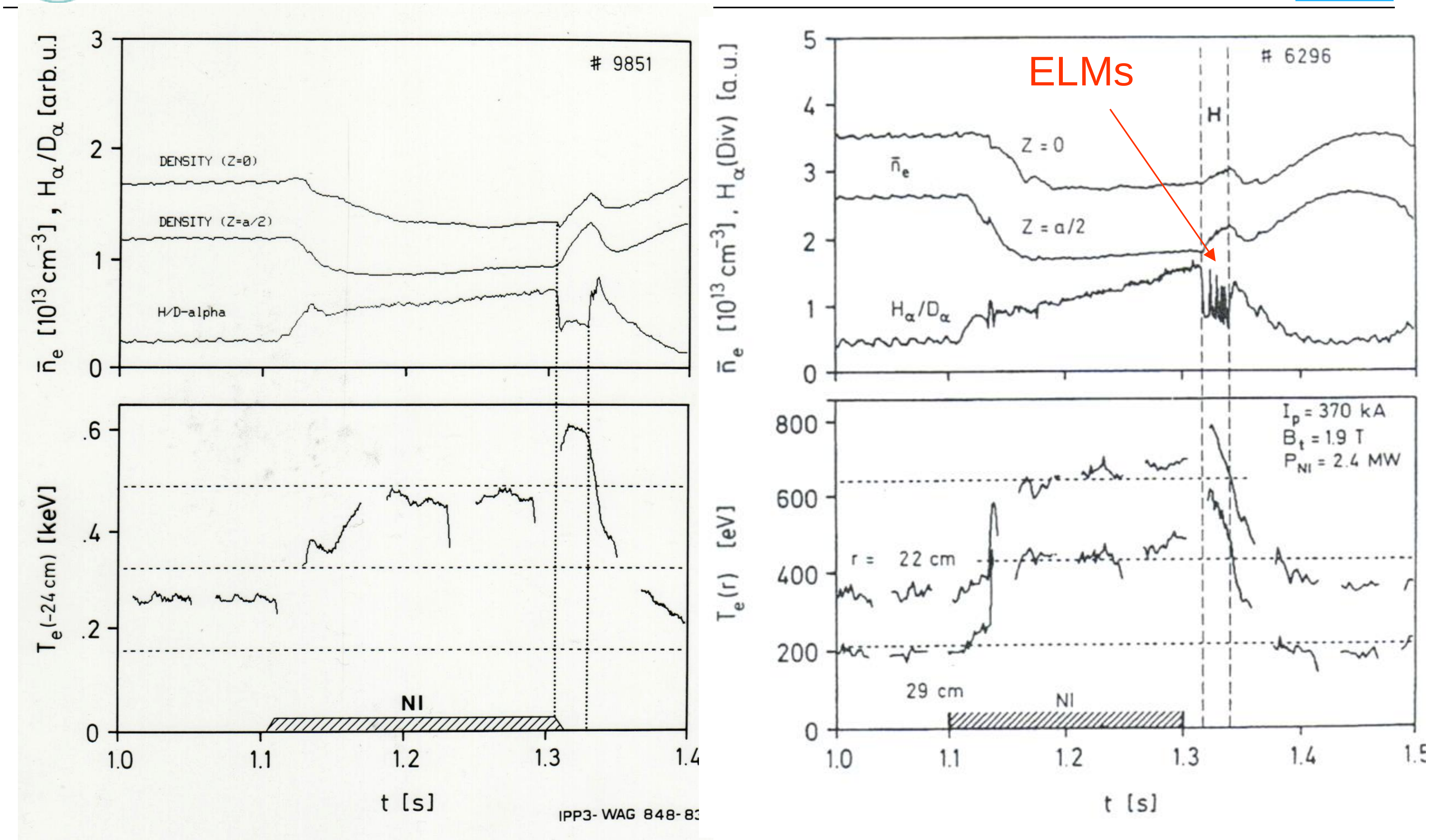

Importance of T_e; theory now: $T_e/\sqrt{L_n}$

Configuration and ion ∇B-drift

The power threshold is low when the ion grad-B-drift is toward the X-point

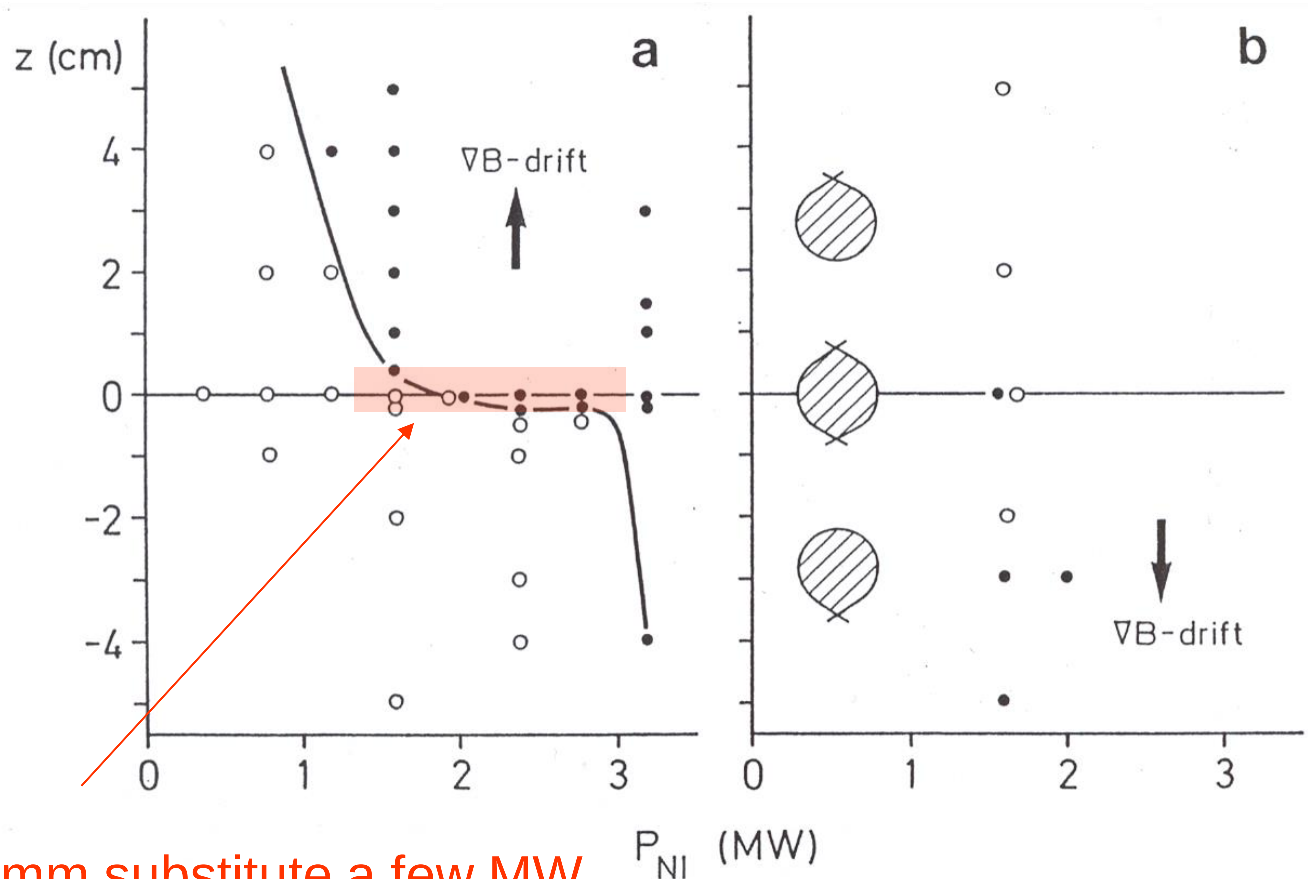

a few mm substitute a few MW

The edge provides a specific transition agent

Therefore, the barrier is locked to the edge

Stellarator H-mode with ELMs

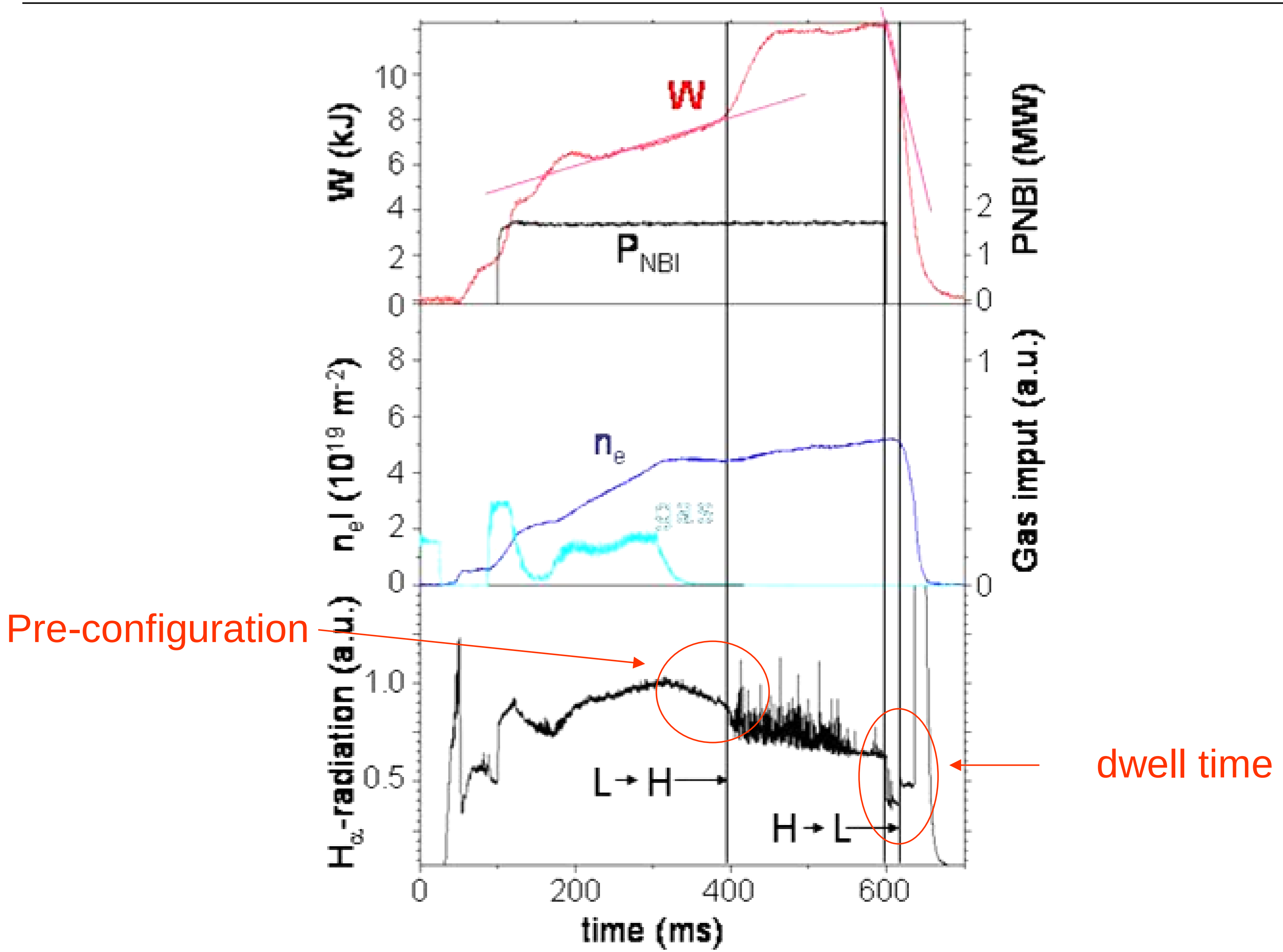

Magnetic characteristics of helical systems

Larger aspect ratio
lower toroidla curvature

Strongly shaped
flux-surface geometry:

TJ-II
heliac

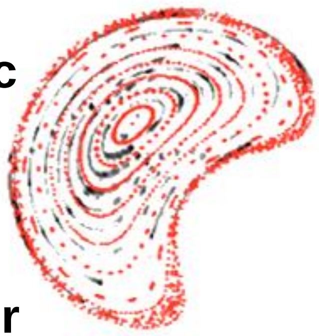

W7-AS, stellarator

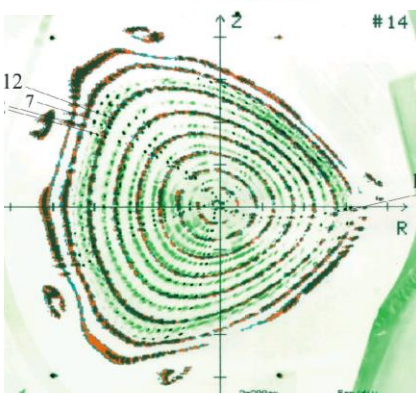

ι-profile:
increases to the egde
global shear S = q´/q

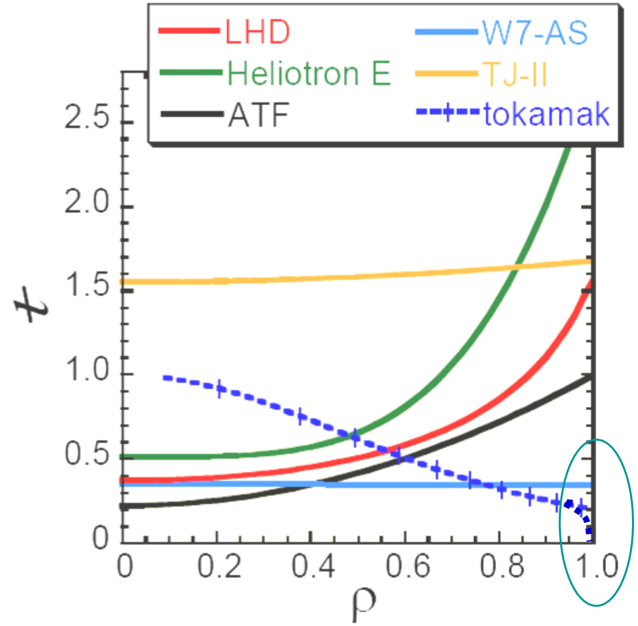

iota =>0
in divertors

Global shear
negative
(Heliotrons – LHD, CHS)
close to zero
stellarators – W7-AS
heliacs – TJ-II, He-1
q, magnetic shear no big role, unlike ITB

H-mode in helical devices

H_a-traces of various devices

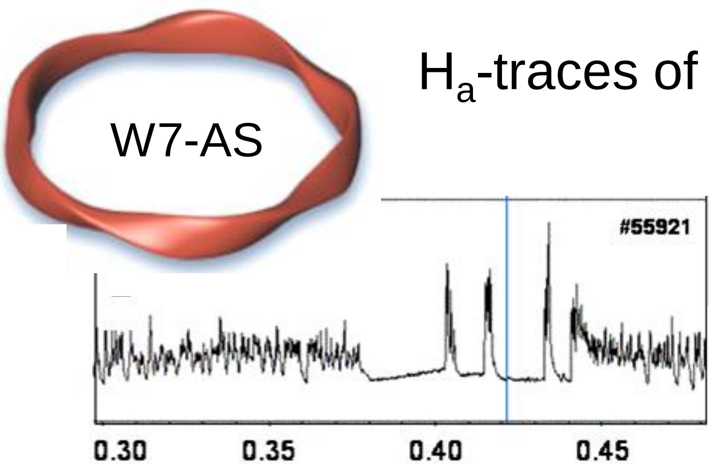

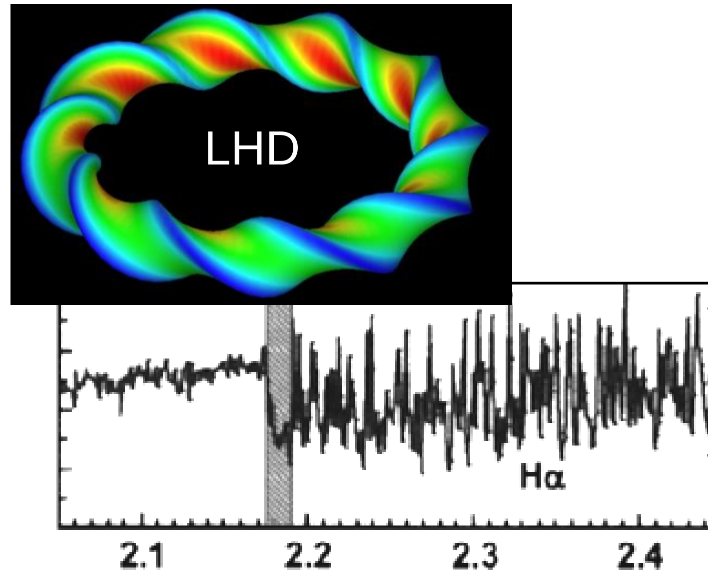

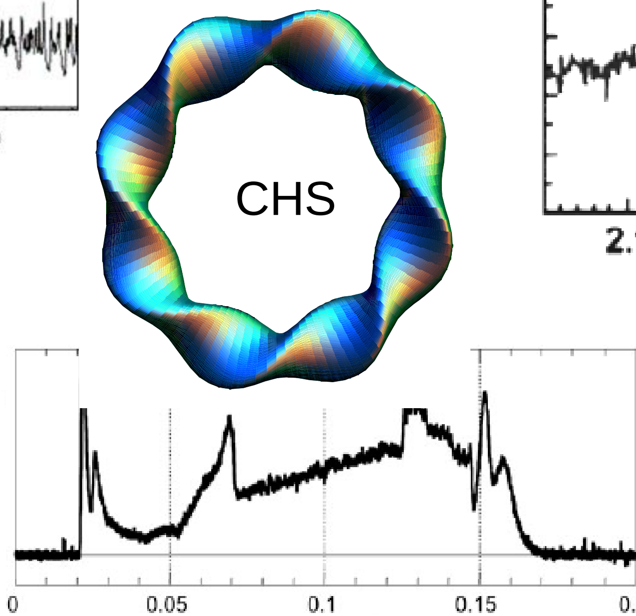

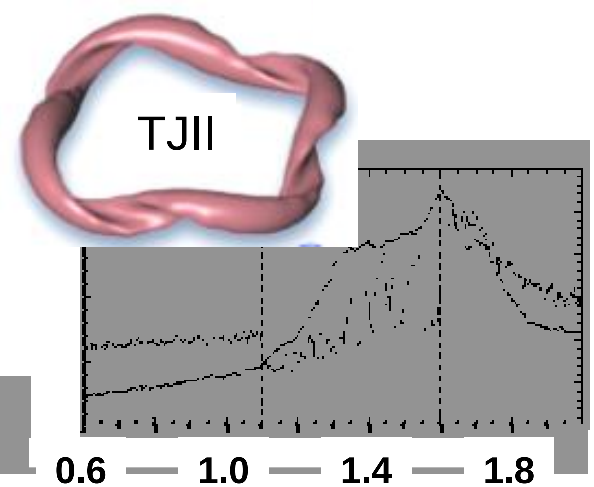

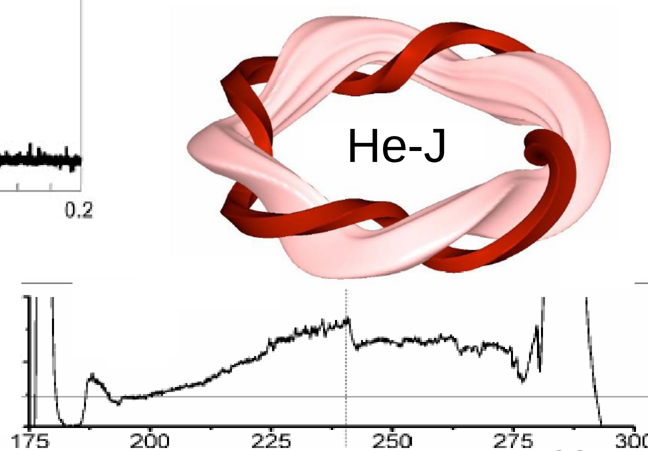

Agreement with tokamak H-mode characteristics

The H-mode develops most easily (lowest power) with separatrix edge

Elmy and quiescent H-modes are possible

The symmetric development is observed: L – H – L

P_{thr} scales with B and n_e (CHS)

Edge gradients increase at the transition

The electric field well deepens at the transition

W7-AS

The edge fluctuation level strongly decreases at the transition

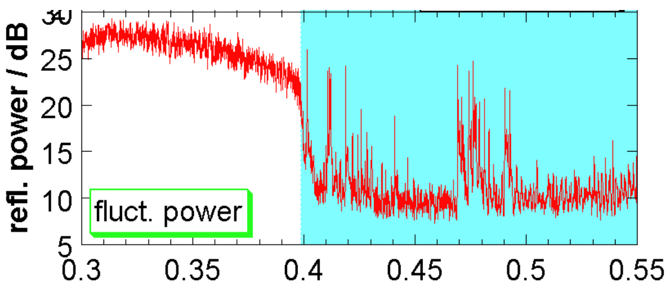

The pivot point of ELMs is 1-3 cm inside separatrix

ELMs last for about 200 μs

$\Delta W/W \sim \Delta N/N \leq 5\%$

Impurity accumulation in H* inspite of broad n_H-profiles

Disagreement, differences

The transition into the quiescent H-mode occurs at a critical (power dependent) density

Operationally, the H-mode is achieved by increasing the density after having increased the heating power (gradual change of control parameter).

H* develops in small iota windows around $\iota \sim 0.5$ (island separatrix)

The transition into the H-mode shows a preceding phase
where E_r already deepens and
the turbulence level generally decreases

The calculated edge bootstrap current is small (ELMs!)

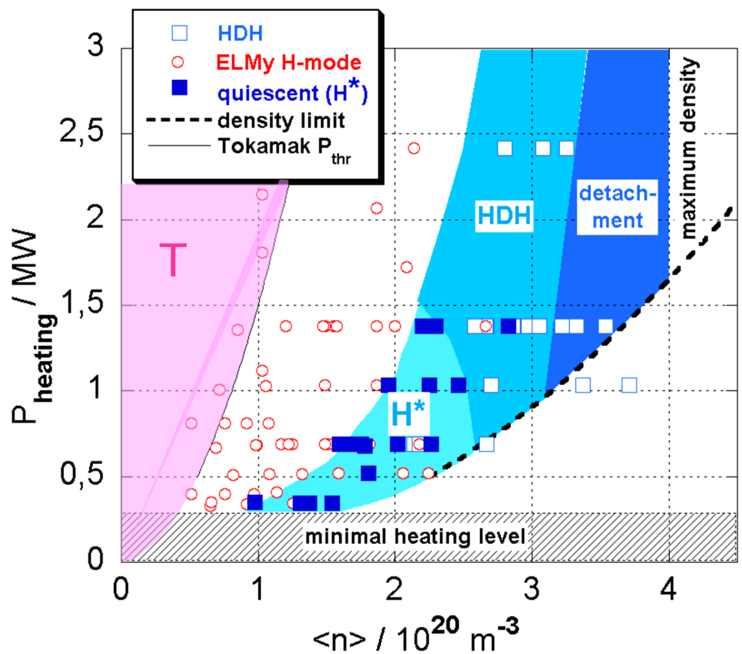

The HDH-mode
(see EDA-mode
of C-Mod!)

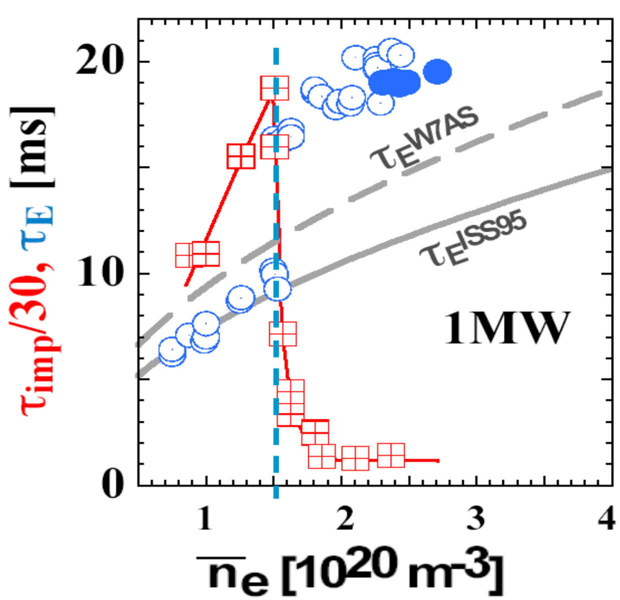

4 Initial understanding

The H-mode as bifurcation

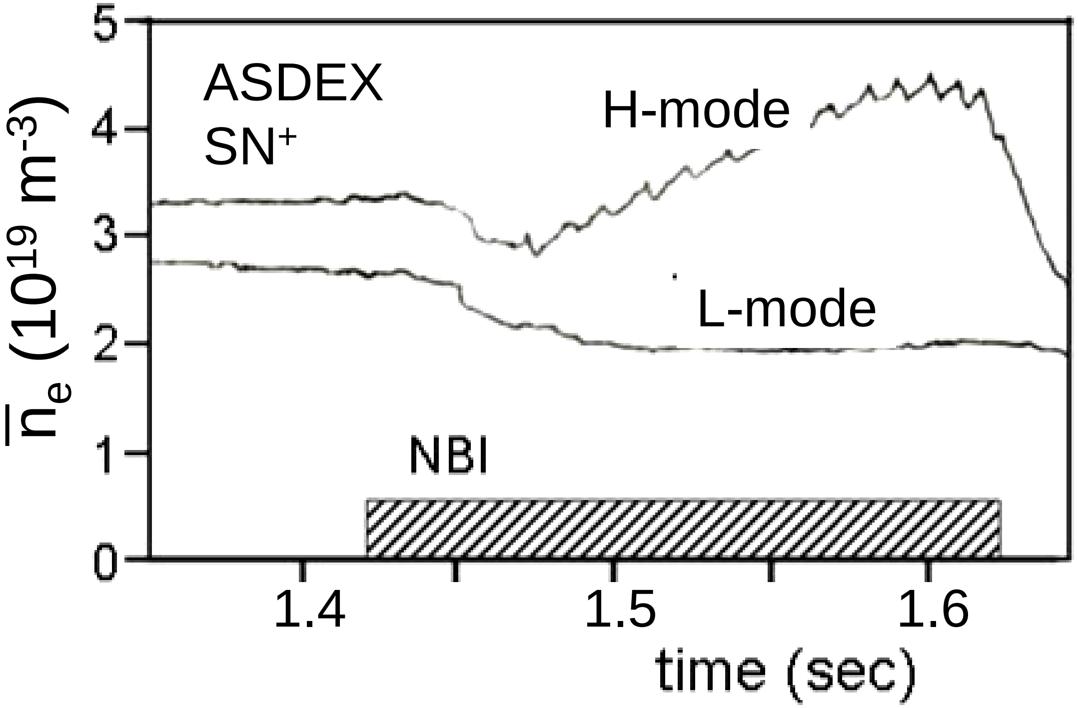

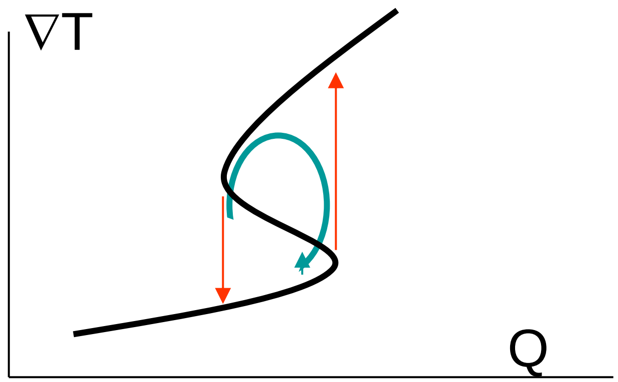

Hysteresis

Limit-Cycle oscillations

Density feedback controlled:
H-mode: density rises though external gas flux to zero
L-mode: density decreases though external gas flux increases

Two confinement branches; space in between not accessible.

Hysteresis, limit-cycle oscillations

Hysteresis: after H-transition, power can be reduced by factor of 2
dwell-time at back-transition: $\Delta t_{H\text{-}L} / \tau_E \sim 0.57$ same for ASDEX, W7-AS
(ASDEX: $\tau_E = 67$ ms; $\Delta t_{H\text{-}L} = 38$ ms. W7-AS: $\tau_E = 28$ ms; $\Delta t_{H\text{-}L} = 16$ ms).

Limit-cycle oscillations:

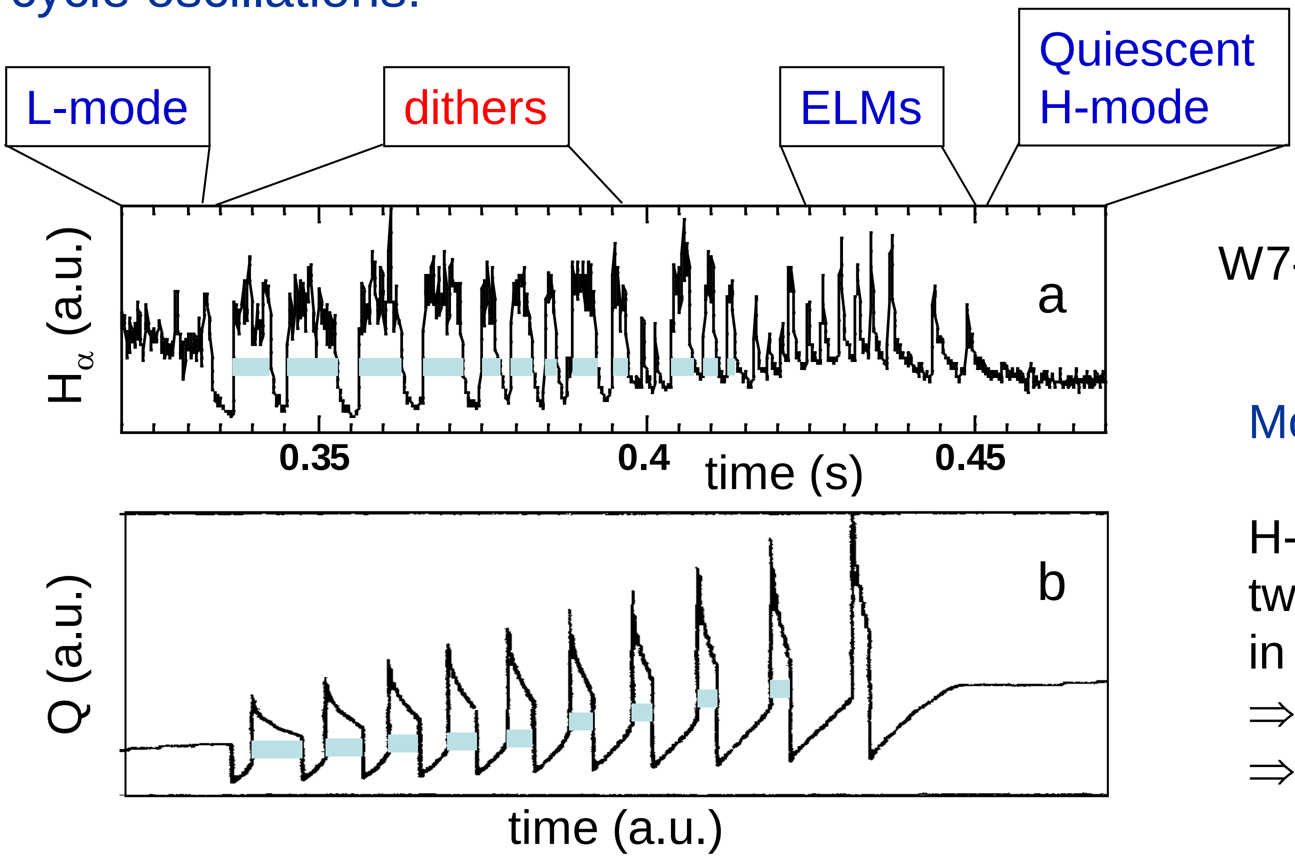

W7-AS

Model by H. Zohm:

H-transition initiates two processes going in opposite direction
$\Rightarrow$ deeper into H
$\Rightarrow$ back to L

Development of an edge transport barrier

SX development with sawteeth after NBI switch-on

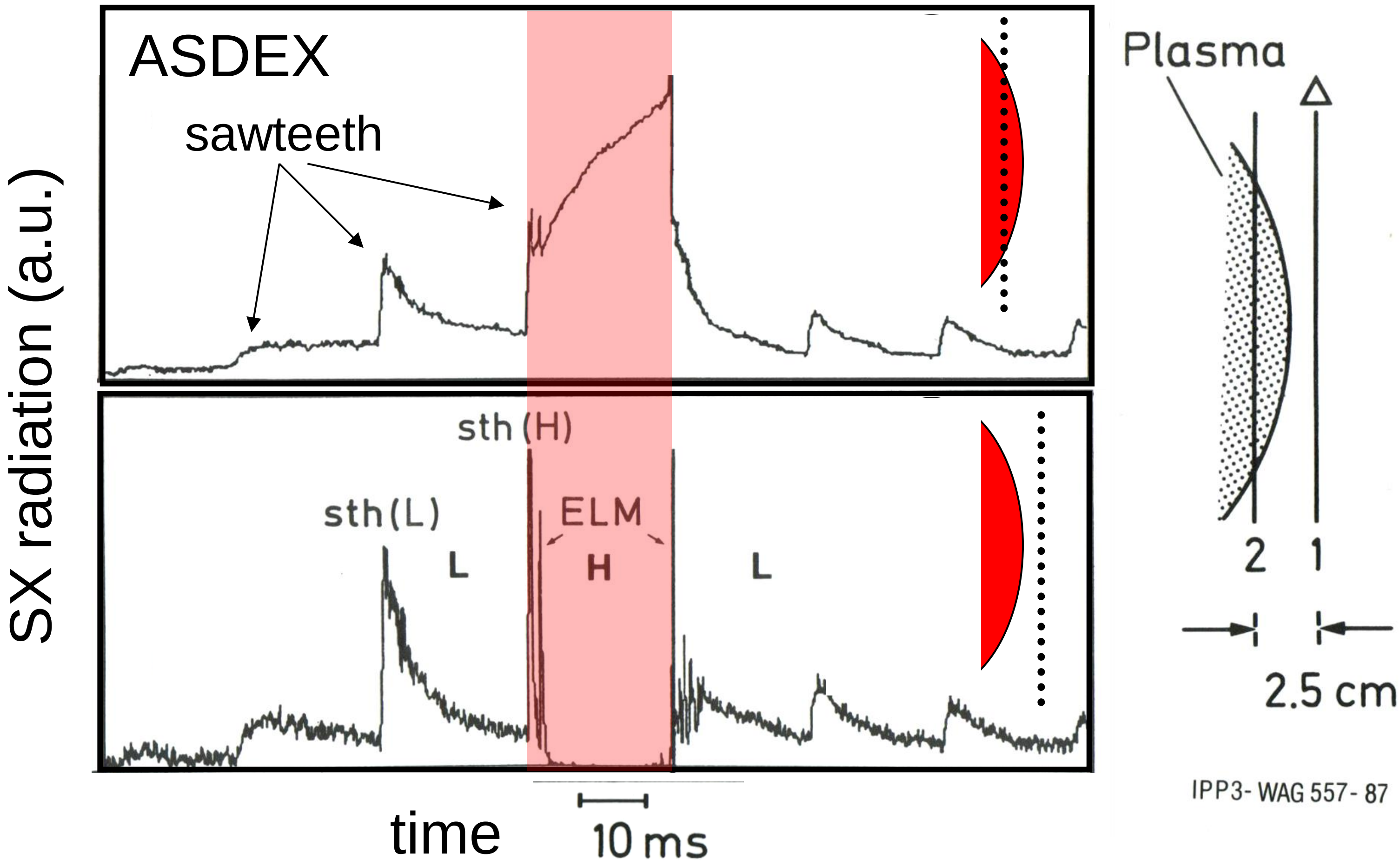

Development of the edge transport barrier

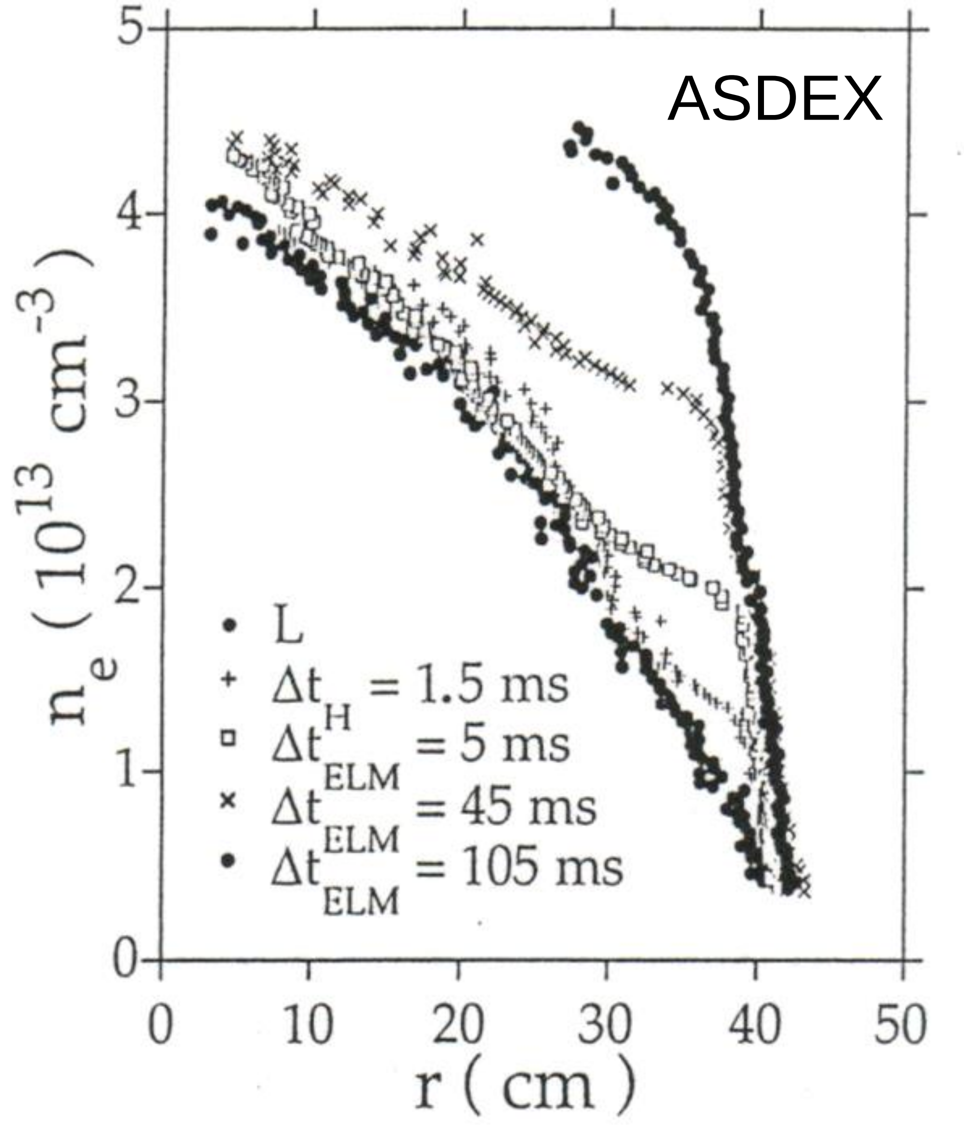

E. Manso, et al.

Reduction of the edge turbulence level

Measurement with CO2-laser scattering at plasma edge

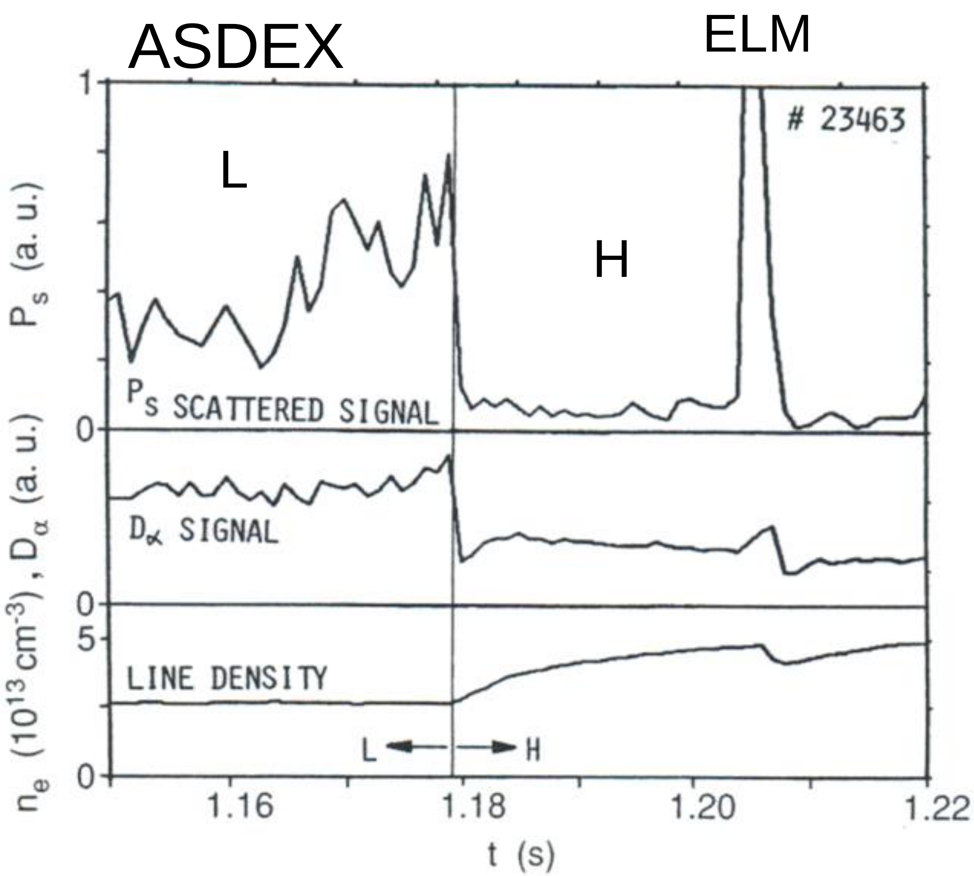

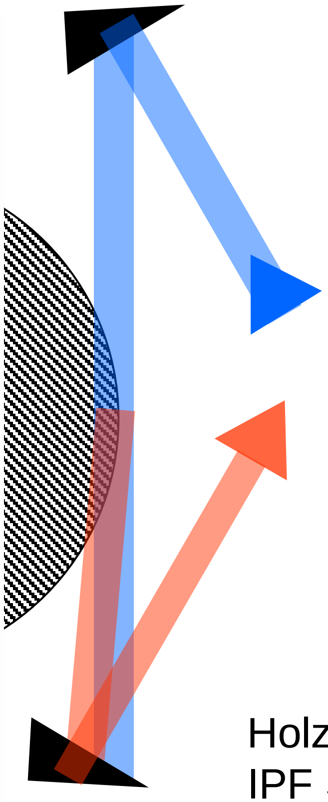

Holzhauer, et al.
IPF Stuttgart

The development of the transport barrier is caused by the reduction of edge turbulence

Reduction of the edge transport

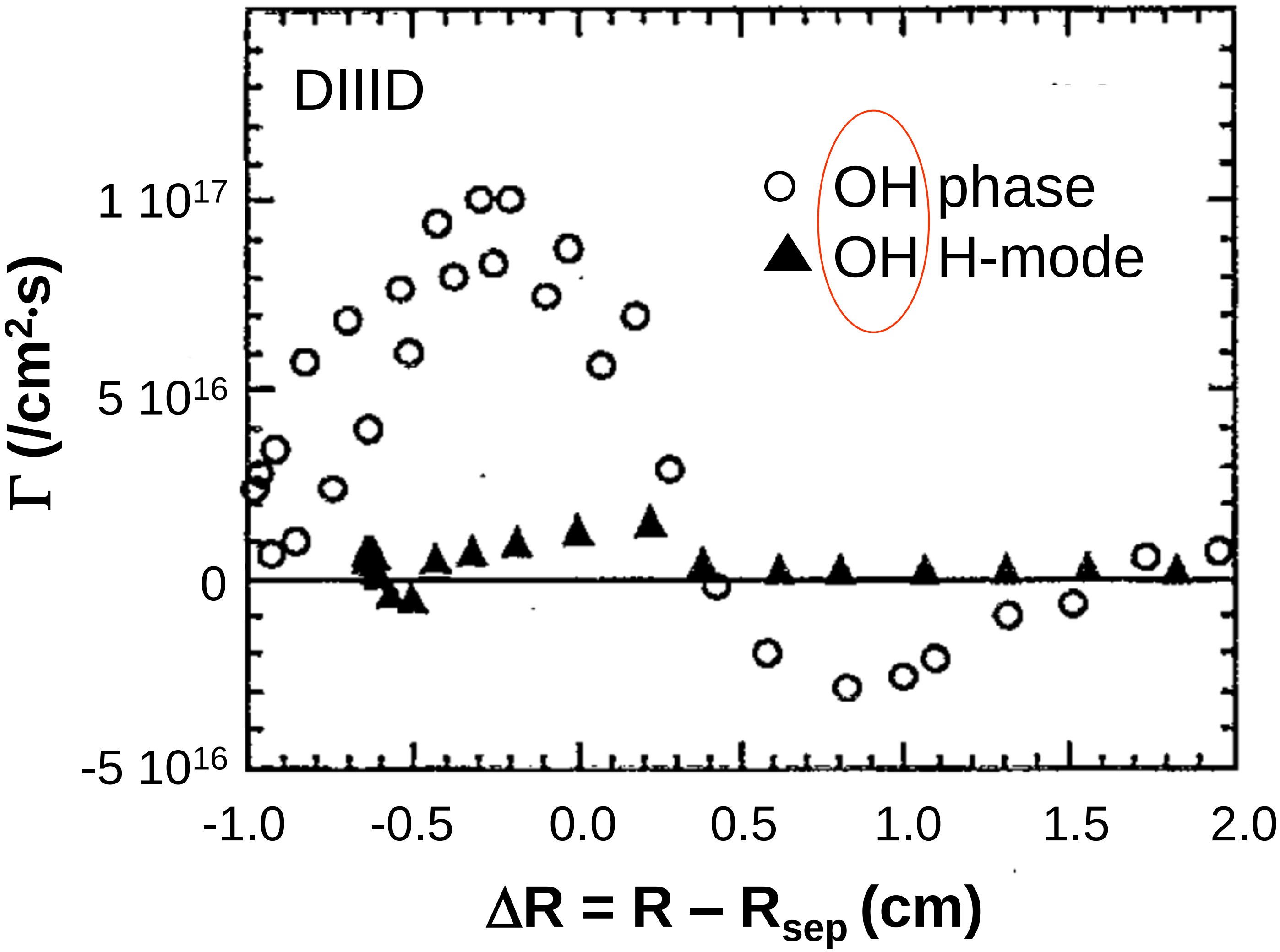

R.A. Moyer et al., Phys. Plasmas

The confinement improvement is caused by a reduction of turbulent fluxes

Summary on initial observations

The H-mode transition results from a balance of supportive and destructive contributions;
The power balance plays a role.

Evidence for source term:

power threshold
dwell time prior to the transition which shrinks with increasing heating power
dwell time after the beam pulse
triggering of H-mode by sawtooth heat pulse
PBP H-mode

Evidence for sink term:

impurity radiation
limiter versus divertor operation
inboard/divertor fuelling versus outboard fuelling

Evidence for role of transport coefficient:

P_{th} is lower for D than H; the same is correct for transport and τ_E.
In stellarators, there is no isotope effect, neither in P_{th} nor in confinement !
Obviously, the isotopic effect is introduced via $\chi_e = f(A_i) \Rightarrow P_{th}(A_i)$

Other process to be discussed now

5 Role of the edge radial electric field

S.-I. Itoh, K. Itoh: Phys. Rev. Letters

R. Groebner, K. Burrell, DIIID-team
Excellent documentation available

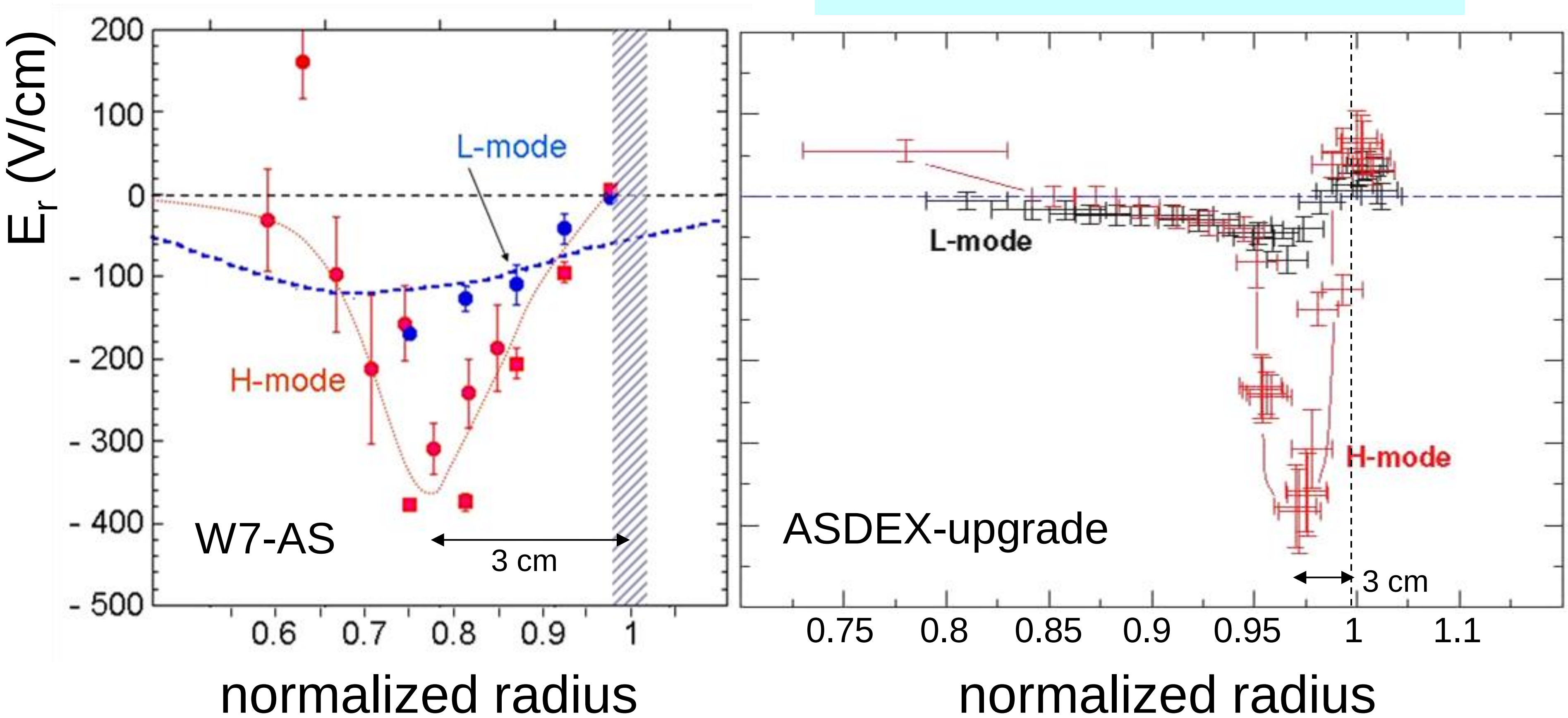

Generic feature of the H-mode: development of an E_r-well inside separatrix

Radial extent of well independent of machine size
In stellarators: E_r-well in the L-phase already quite deep => $P_{th}^{STELL} < P_{th}^{TOK}$

Changes in edge flow direction

ASDEX

L-mode

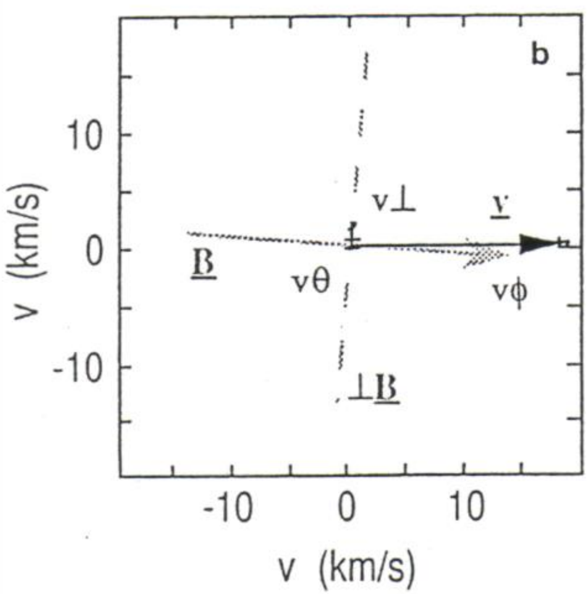

H-mode

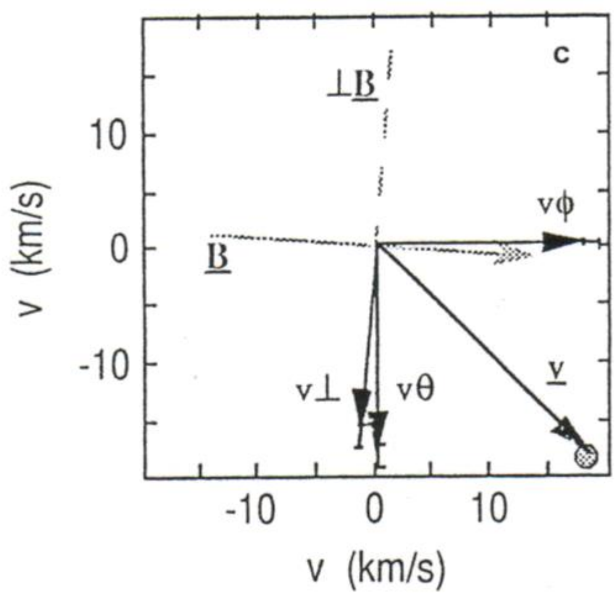

H-mode, B_{tor} reversed

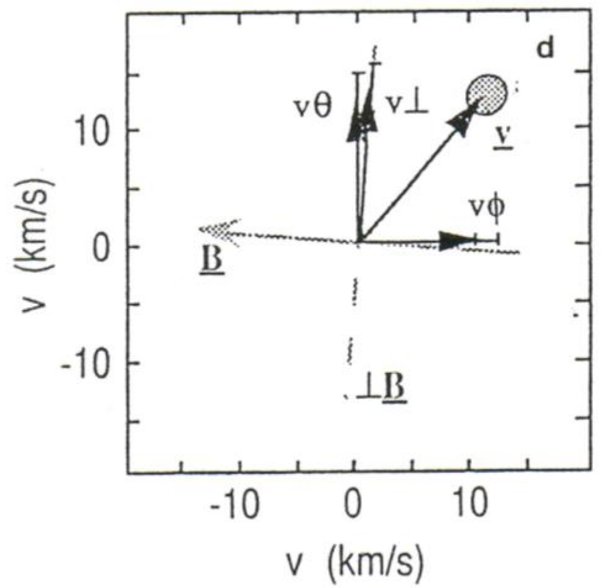

Causality between E_r and transport

Polarisation probe studies on TEXTOR

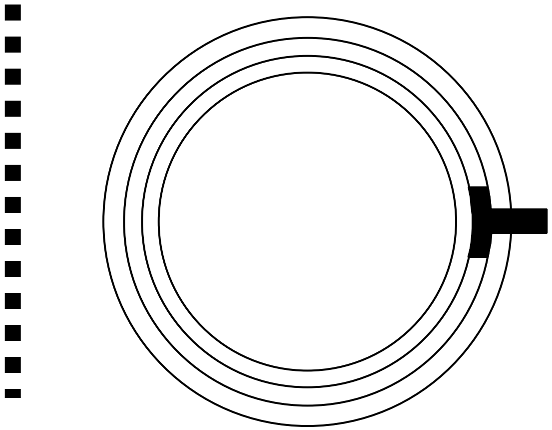

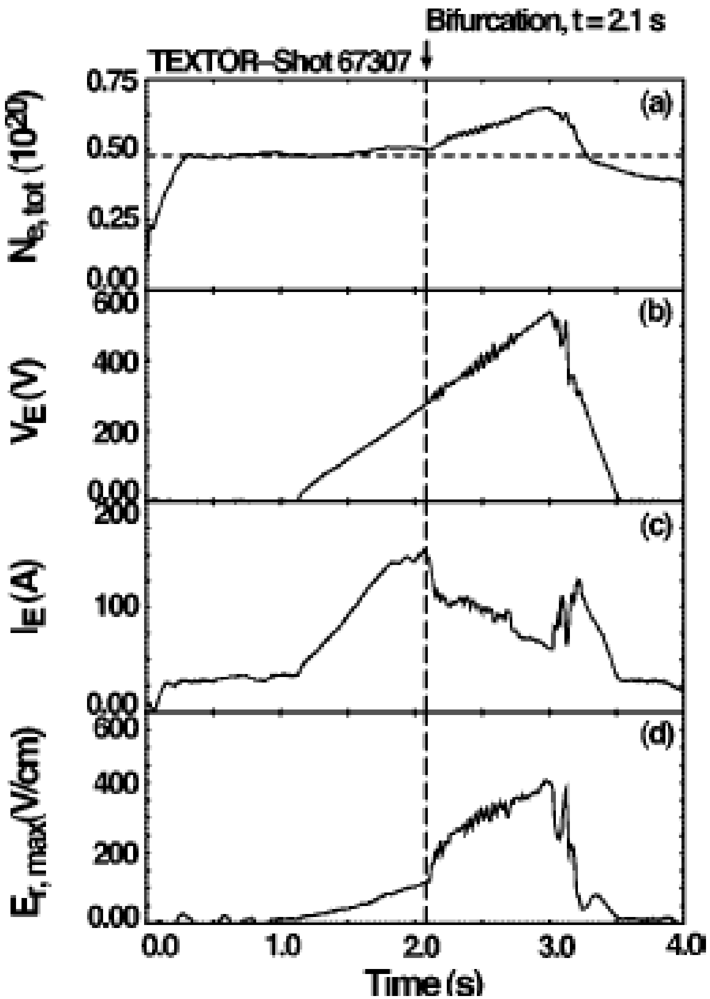

Use of biasing probe makes E_r to a control parameter

Induced H-phases

J. Boedo et al., Nucl. Fusion

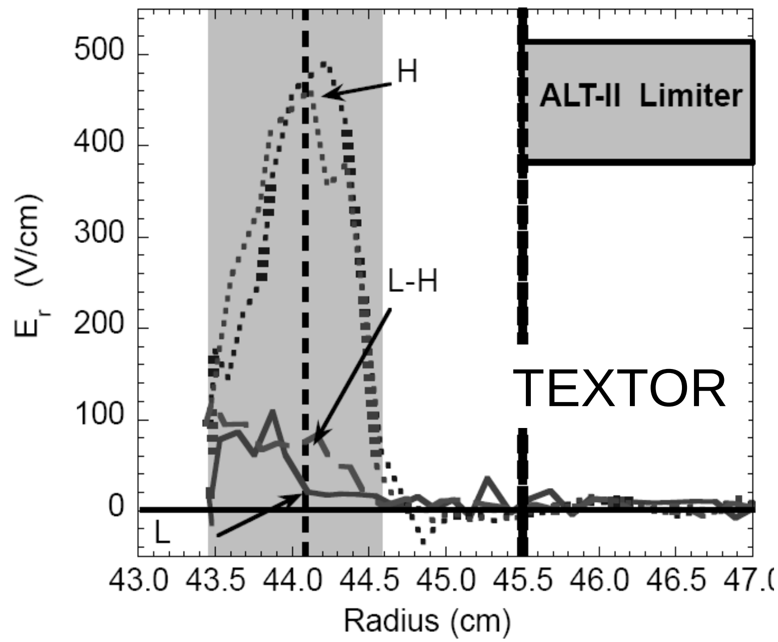

The fluctuations decrease gradually!

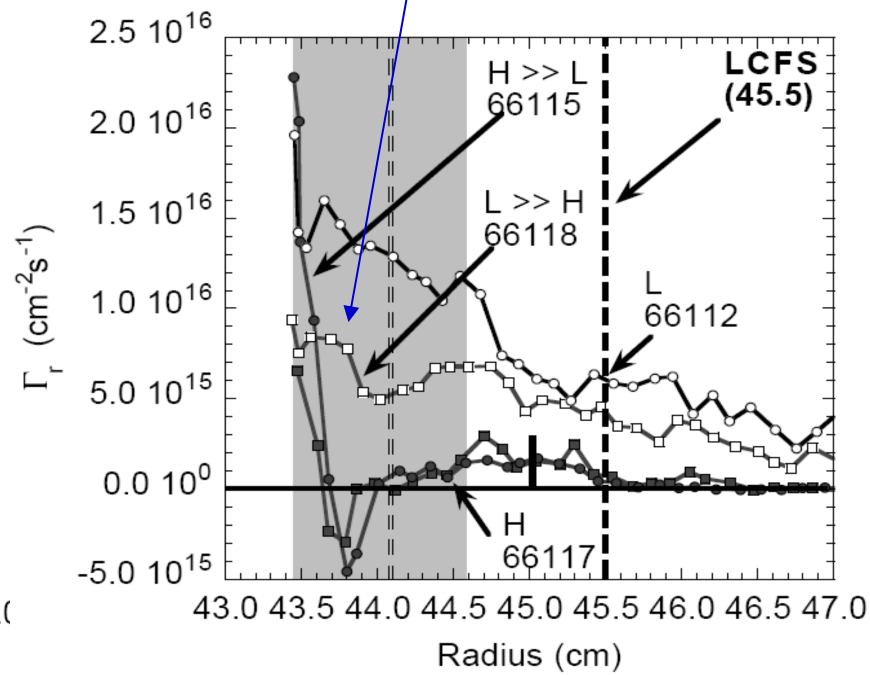

Within the E_r-well, the turbulent transport is quenched

The E_r-field (gradient) is the cause of the edge transport barrier

Is there a more continuous relation between $\Gamma_{turbulent}$ and E_r?

Shear flow decorrelation of turbulence

H. Biglari, P. H. Diamond, P. Terry

$\omega_{E\times B} > \gamma_{lin}\,(\Delta\omega_D)$ Shearing rate: $\omega_{E\times B} \approx \dfrac{1}{B_{tor}}\dfrac{\partial E_r}{\partial r}$

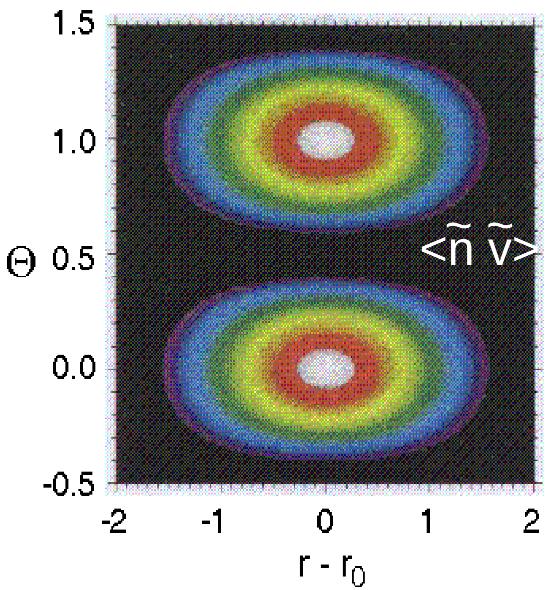

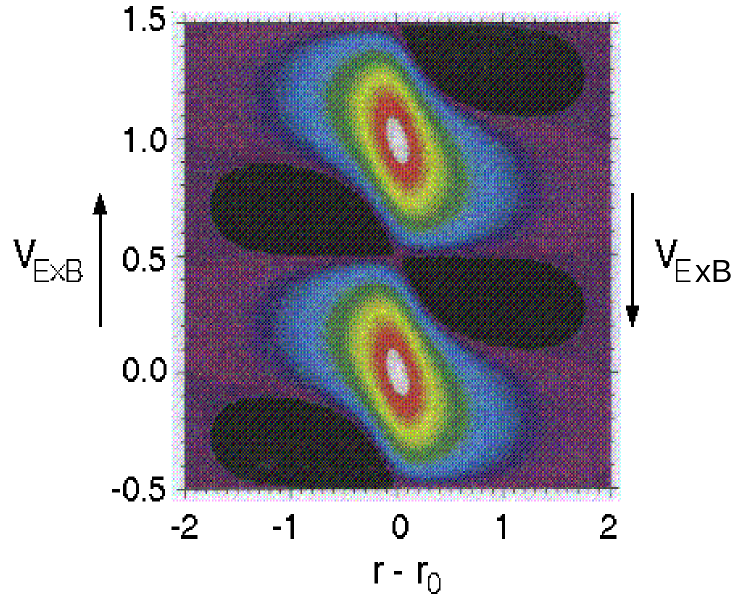

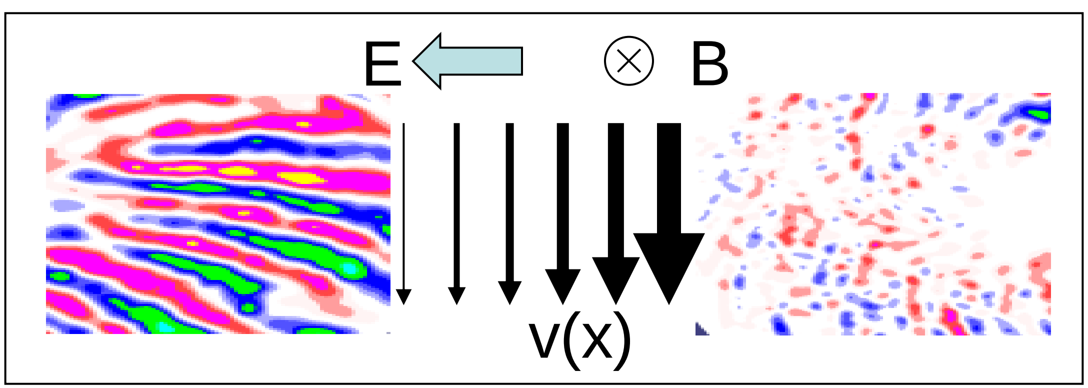

Turbulence becomes more isotropic

Radial size scales reduced

Experimental confirmation of shear flow decorrelation

Conditions for flow-decorrelation

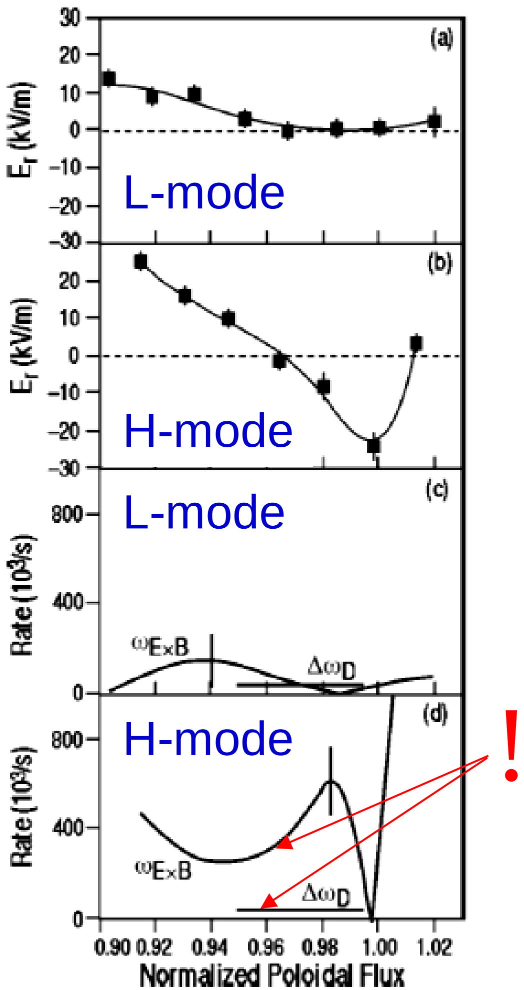

Reduction of radial correlation length

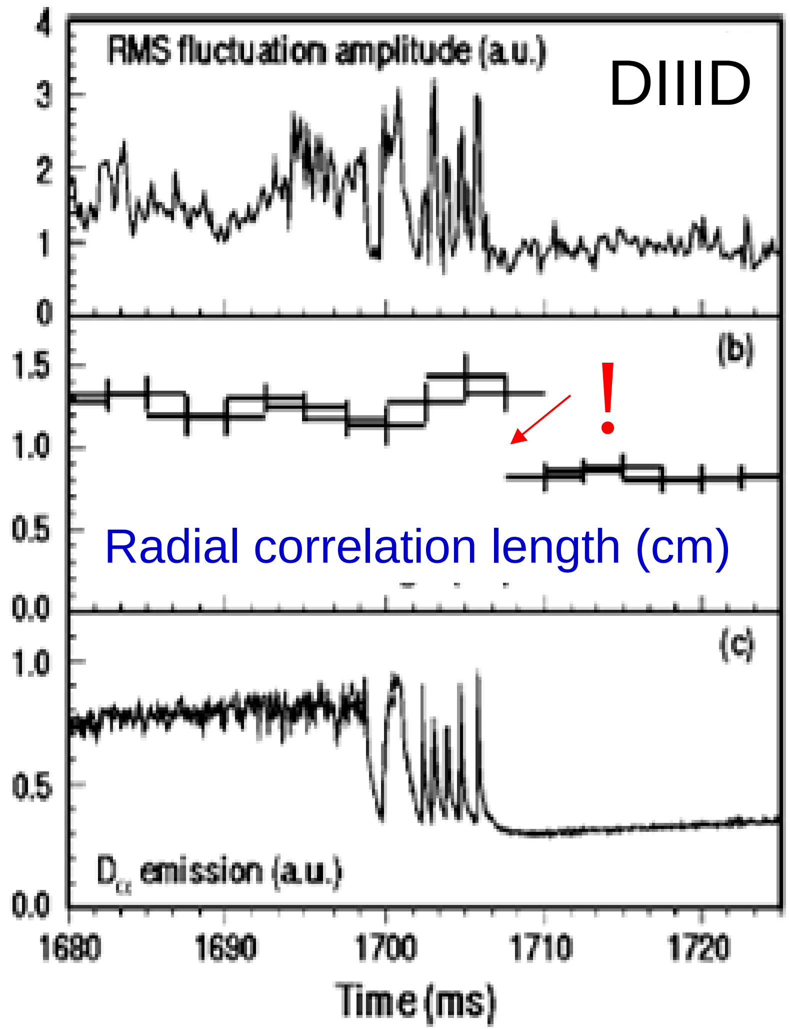

Probe (Textor):

$\nabla|E_{r,crit}|$ = 50-80 V/cm^2

DIII-D:

$\nabla|E_{r,crit}|$ = 50-100 V/cm^2

W7-AS:

$\nabla|E_{r,crit}|$ ~ 90 V/cm^2

K.H. Burrell, Phys.Plasmas

Modelling of shear-flow decorrelation

Gyrokinetic particle simulation of plasma microturbulence

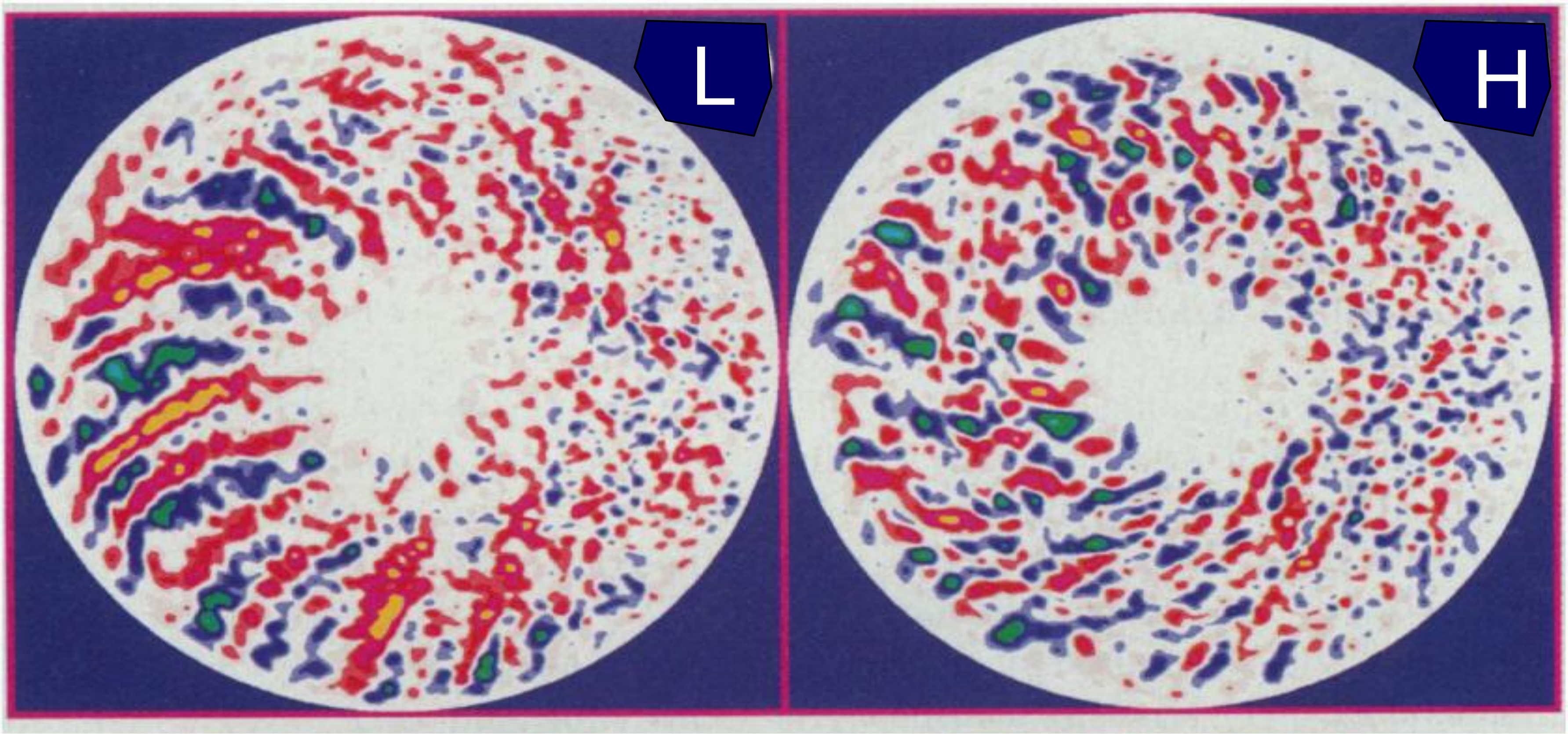

∇B

Z. Lin at al., Science

6 The Origin of E_r at the edge

2D:

Fluxes are intrinsically ambi-polar and transport coefficients do not explicitely depend on E_r

$\langle j_r \rangle = 0$, independed of E_r

3D:

$\langle j_r \rangle = 0$, ensured by $\Gamma_e = \Gamma_i$: enforced ambi-polarity

$$\Gamma = -D_1(E_r)\,n\left\{\frac{1}{n}\frac{\partial n}{\partial r} - q\frac{E_r}{T} + \frac{D_{12}}{D_{11}}\frac{1}{T}\frac{\partial T}{\partial r}\right\}$$

$$E_r = \nabla p_i / en + (D_{12}/D_{11} - 1)\,\nabla T_i$$

Stellarator ambi-polarity is characterized by bifurcations:
electron/ion roots
E_r changes with the gradients ($O(\tau_E)$)

The composition of E_r

Radial force balance: $E_r = \nabla p_i / e n_e - v_\theta B_\phi + v_\phi B_\theta$

Tokamak: 2D

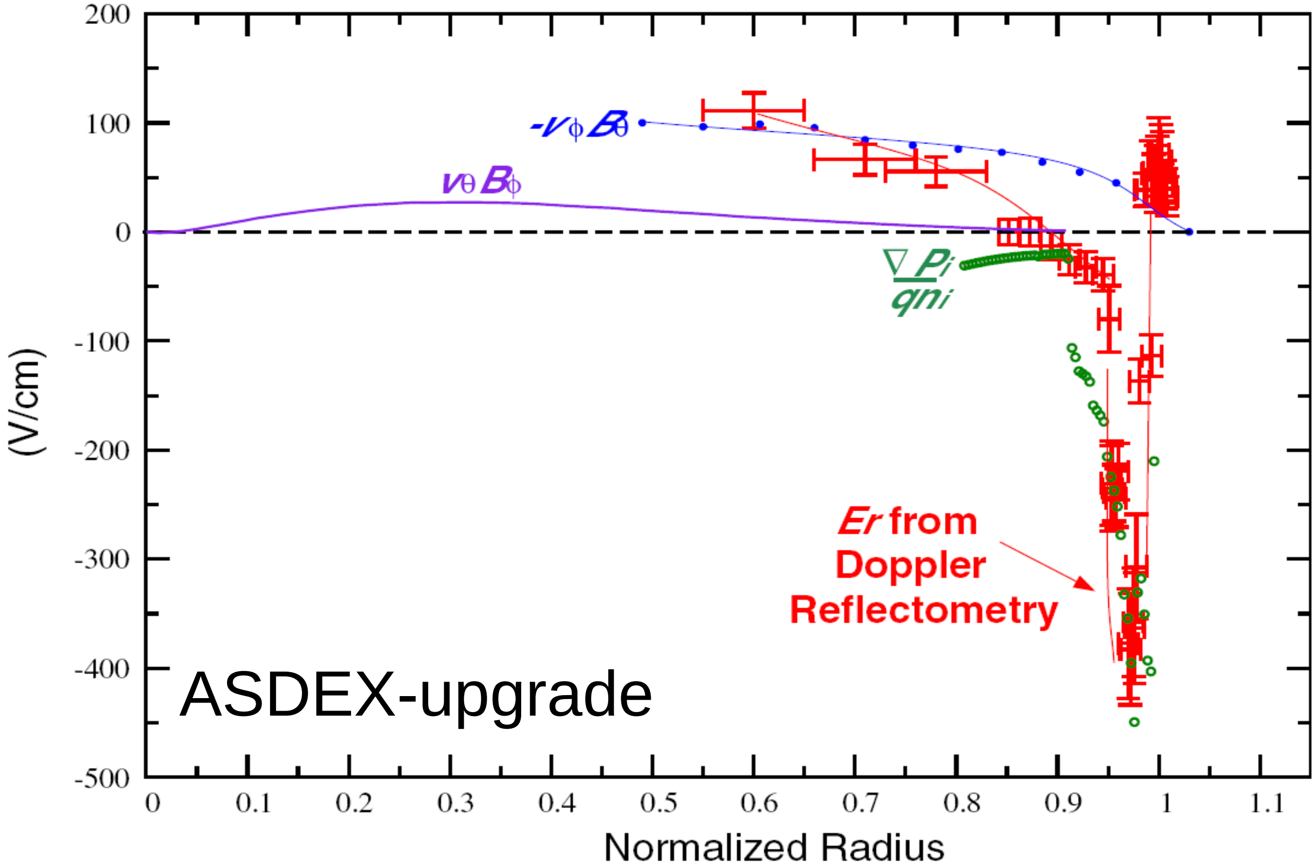

In a fully developed H-mode: $E_r(a-\delta)$ given by ∇p_i

∇p_i plays an important role: it stabilises the developed H-mode

co-NBI: unfavourable conditions

Causality between E_r and ∇p_i

TEXTOR: H-mode induced by polarisation probe

E_r is oscillating

n_e ($\mathrm{grad}p_i$) also oscillates

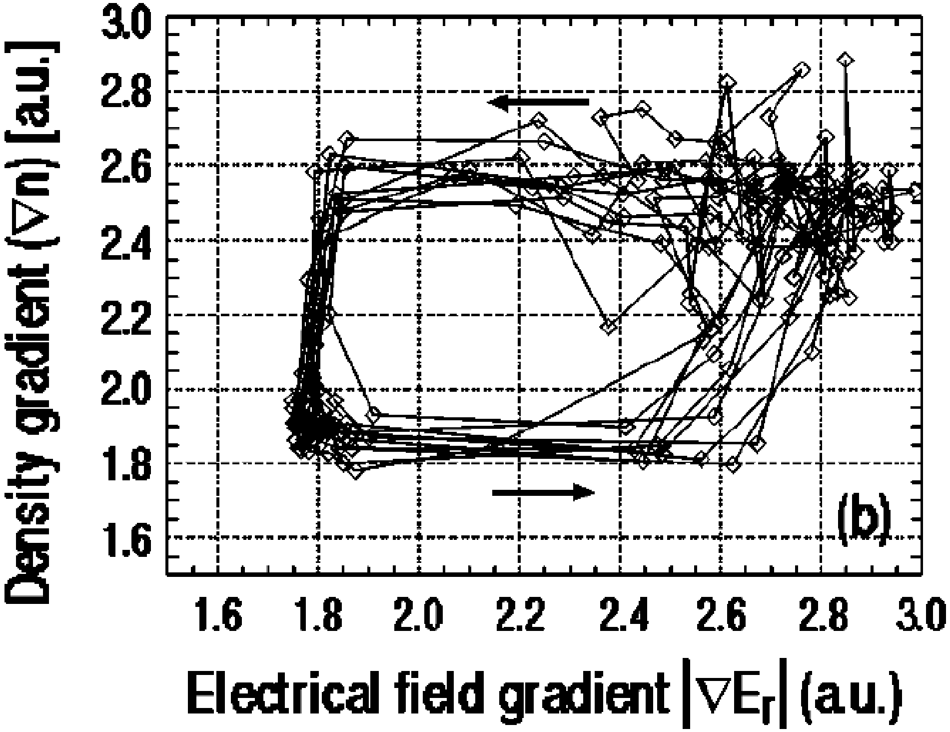

Analysis done by K.H. Burrell, Phys. Plasmas

Causality: ∇E_r leads n_e by about 5 ms

Temporal characteristics of L $\Rightarrow$ H

R. Groebner, K. Burrell, R. Moyer, DIIID-team

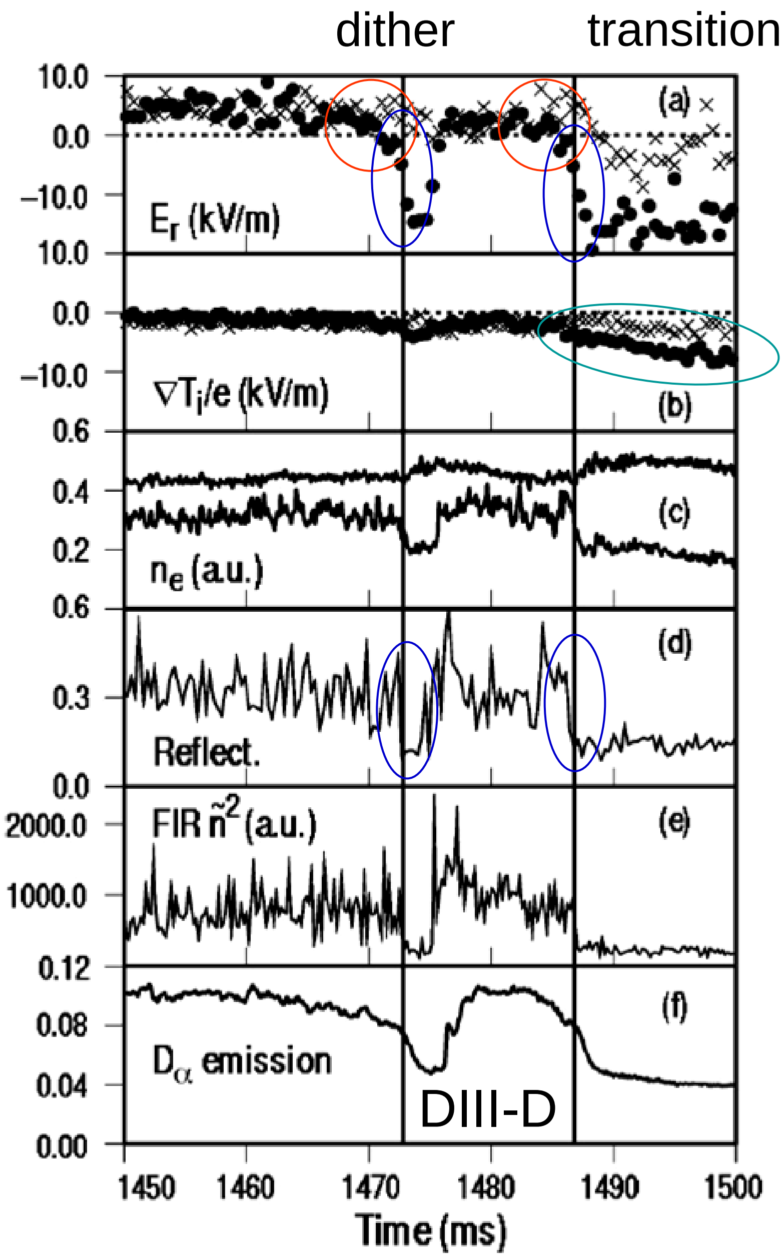

There is a pre-phase

Jump of E_r at the L=>H transition ($\tau << \tau_E$)

T_i changes slowly

The turbulence level drops joinly with E_r

JFT-2M: transition within 12 μs

R.A. Moyer et al., Phys.Plasmas, 2, 2397, 1995

Temporal characteristics of the back transition H $\Rightarrow$ L

W7-AS: back transition

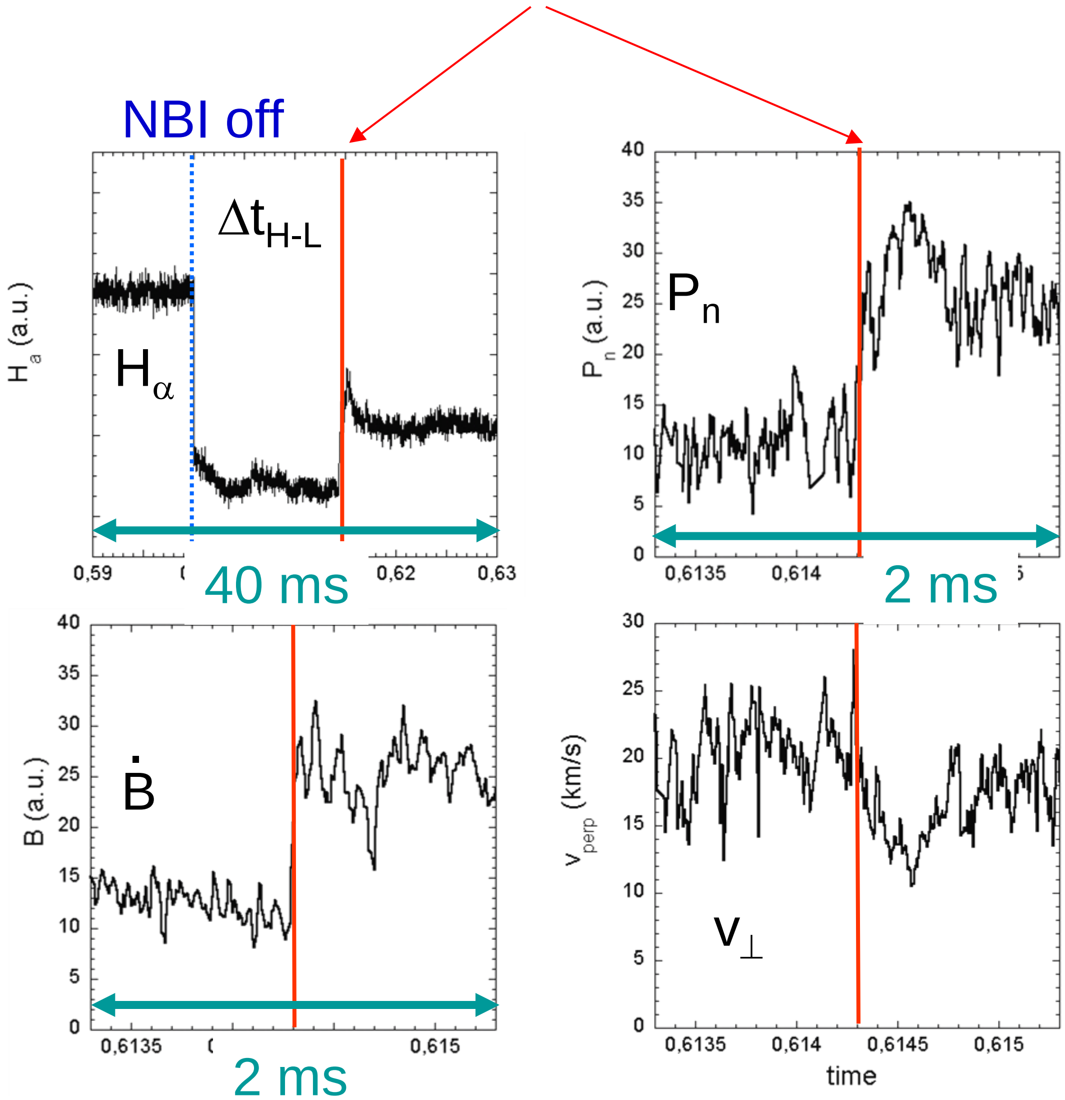

Scattering power of reflectometry

From Doppler-reflectometry

back transition: 10 μs

P_n and $v_\perp$ show a more complex transition pattern

Jump in E_r at the back transition

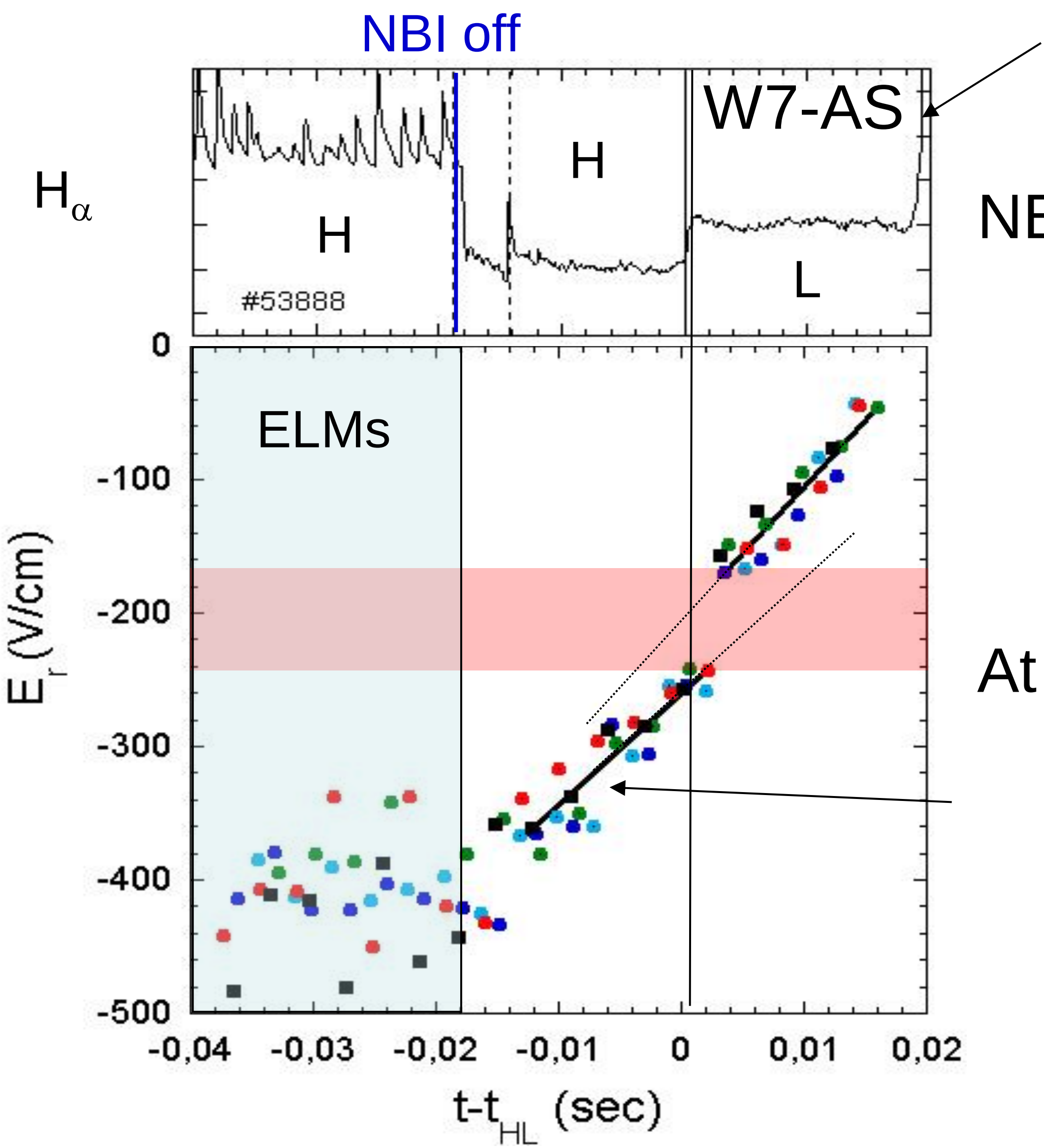

NBI-off:
- fluctuations increase
- E_r increases
- ∇p_i is constant in this phase

At back transition
- jump in $\Delta E_r \sim 80$ V/cm
- $\Delta t < 1$ ms
- bifurcation occurs in E_r

There a continuous relation between $v_\perp$ and $\tilde{n}$

Back transition

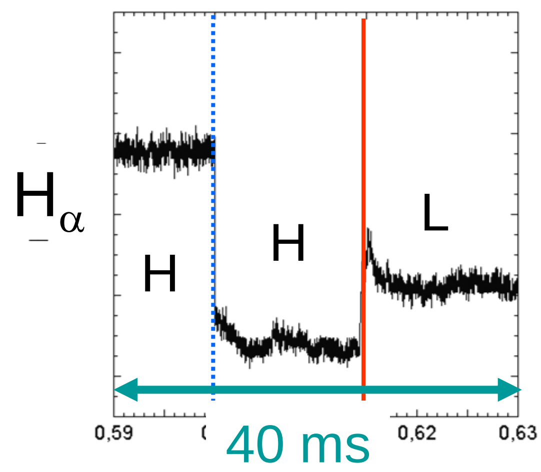

Variation of the scattering power P_n (logarithmic scale) with $E_{r,min}$

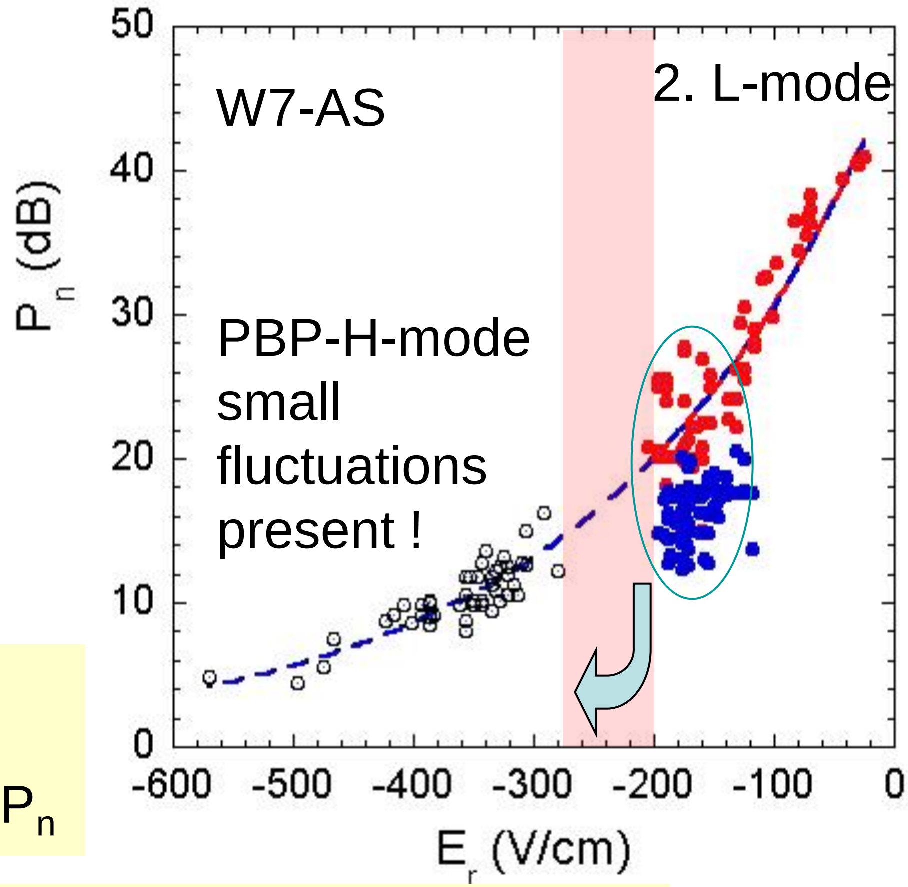

Continuous variation of P_n with E_r

The jump in E_r may cause the jump in P_n

Asymmetry in L=>H versus H=>L: different edge pressure profiles

L-mode equilibrium ⇔ L-mode transport at H-mode profiles

Role of the v×B-term

Radial force balance: $E_r = \nabla p_i / e n_e - v_\theta B_\phi + v_\phi B_\theta$

$v_\phi B_\theta$ introduces the toroidal momentum balance

co-NBI obstructs the transition
(DIIID: P_{th} lower with ctr-NBI)

~ 0 in helical systems (edge ripple)

Role of the v×B-term

$v_\theta B_\phi$ Introduces the poloidal momentum balance

Several concepts and models developed

Ion loss model

would explain short time scales!

but: L-H transitions in large range of ν^*

Physics of poloidal viscosity

W7-AS: strong relation between edge field structures and H-mode window

W7-AS: M_θ ~ 2-3

Tohoku heliac: μ beyond tor. resonance

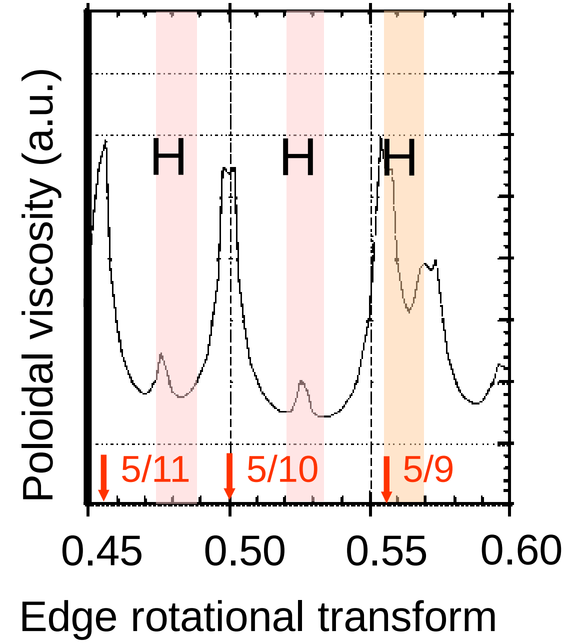

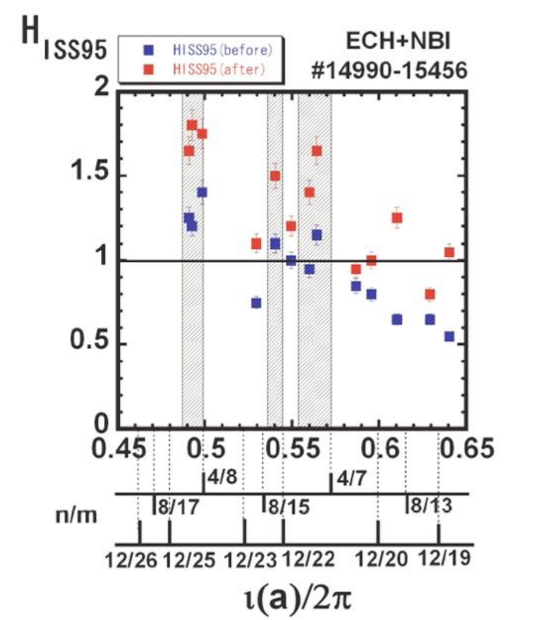

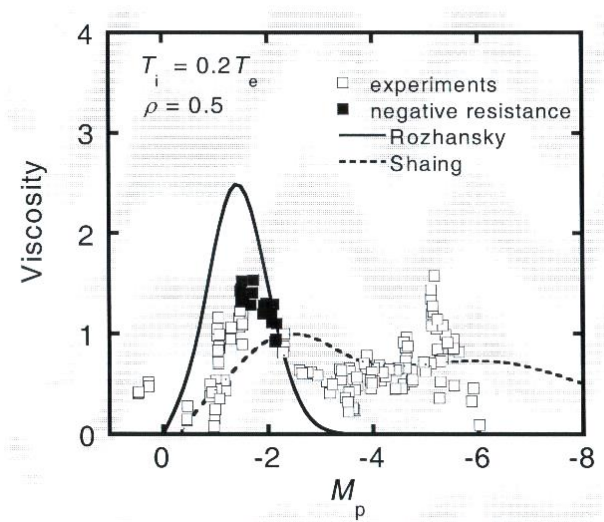

Flow drive originating from SOL flows

Addressing the effect of the configuration onto P_{th} (ion-grad B drift, $B \times \nabla B$)

The turbulent flow from the plasma into the SOL at the low-field side

SOL-flows from transport, PS-flows, $E_r \times B$ -flows (E-field positive in SOL)

SOL-flow dissipates across separatrix (C-Mod)

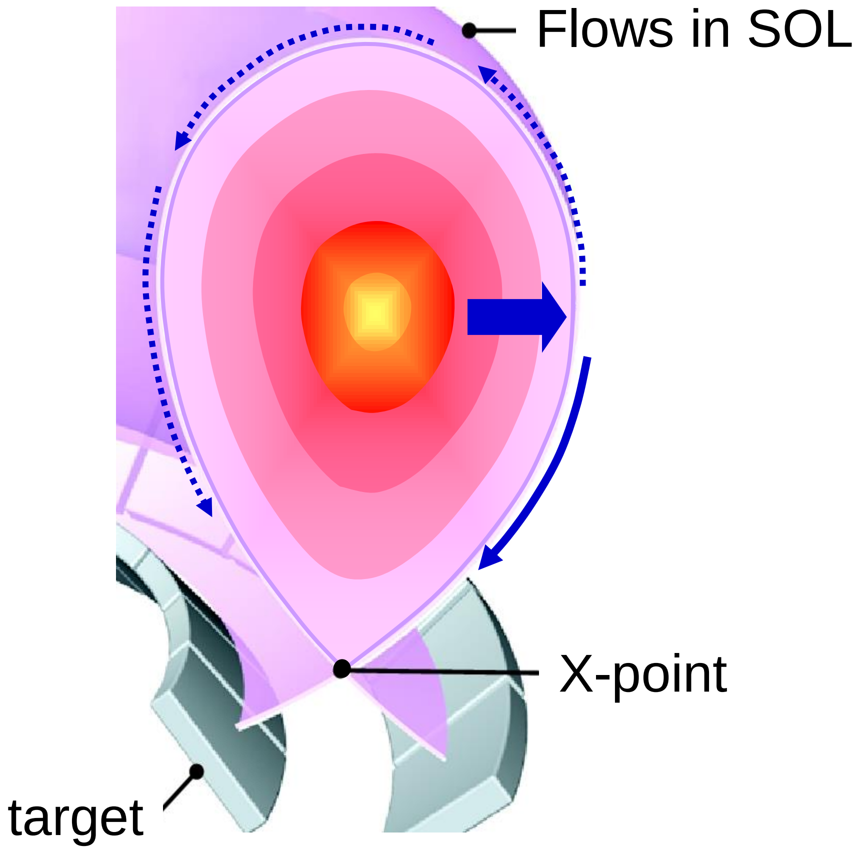

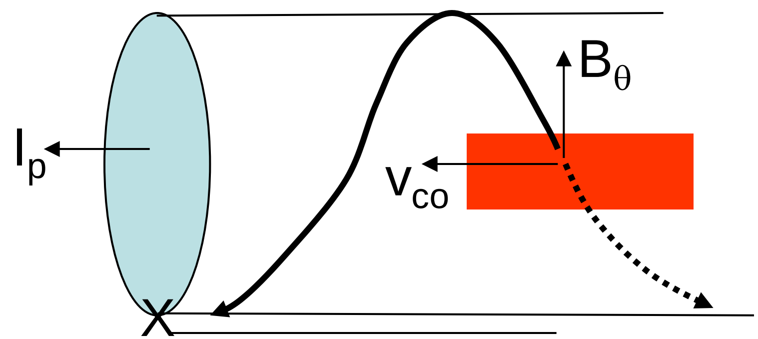

SN+: rotation in co-direction; E_r^{SOL} more positive

SN-: rotation in ctr-direction: E_r^{SOL} less postitive

Difference in E_r^{SOL} : 100-200 V/cm

Short detour to the planets

Jupiter

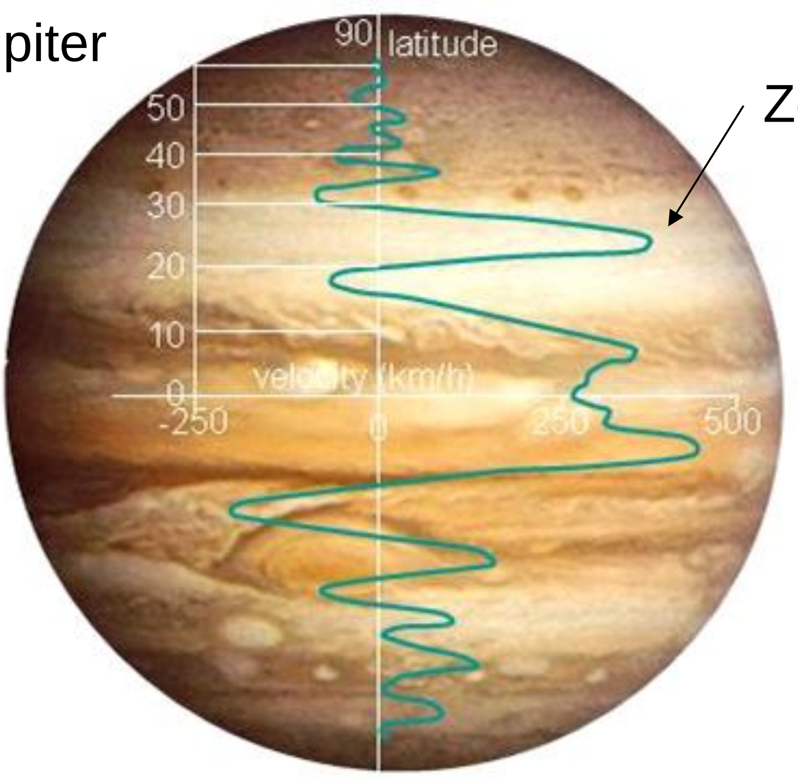

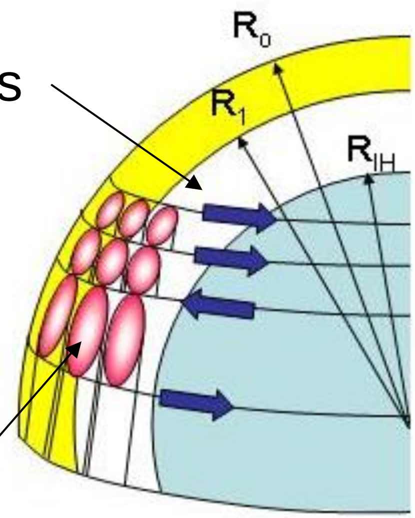

Formation of large-scale flows (zonal flows) from turbulence via RS.
ZFs are sheared flows perpendicular to the turbulence driving gradients.
Observd in laboratory experiments,
the sonic wind in gases,
meandering flows in oceans, Jet streams, in the ionosphere
e.g. Rossby waves (Coriolis force instead of Lorentz force)
in the sun

Reynolds stress and Zonal flows

Poloidal force balance: $0 = j_r B/n_i - m_i \mu_\theta v_{\theta i} + m_i \partial/\partial r\, (\langle \tilde{v}_{ri} \tilde{v}_{\theta i} \rangle)$

Reynolds stress leads to steady-state flow

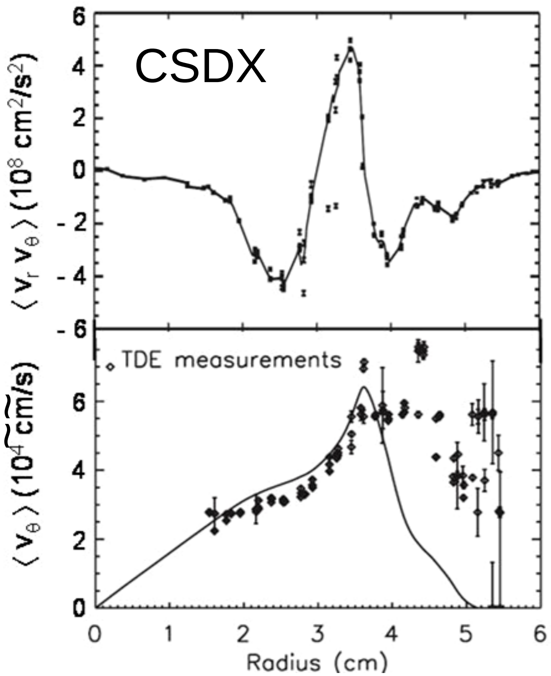

Transient 3-wave coupling at the transition

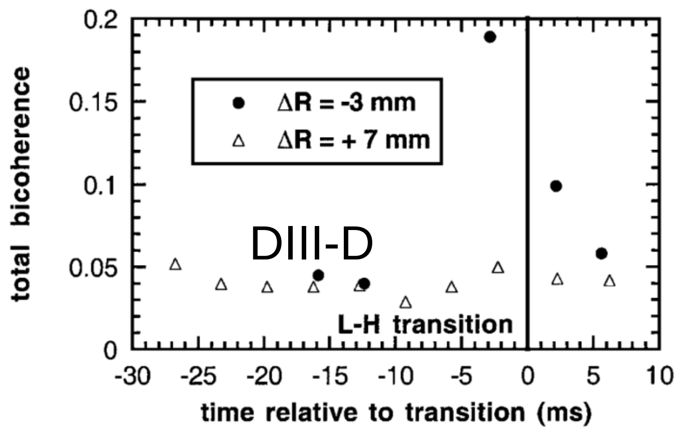

Measurement of a Zonal Flow

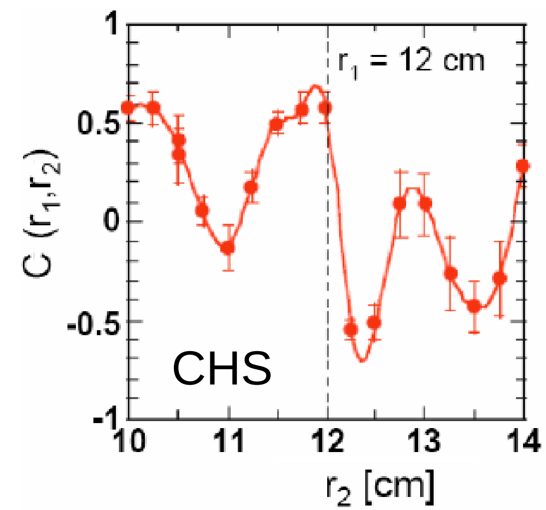

Evidence for the RS mechanism in plasmas

ZF demonstrated

C. Holland et al., Phys. Rev. Letters
R. A. Moyer et al., Phys. Rev. Letters
A. Fujisawa et al., Phys. Rev. Letters

The role of Zonal flows in L-H Transitions

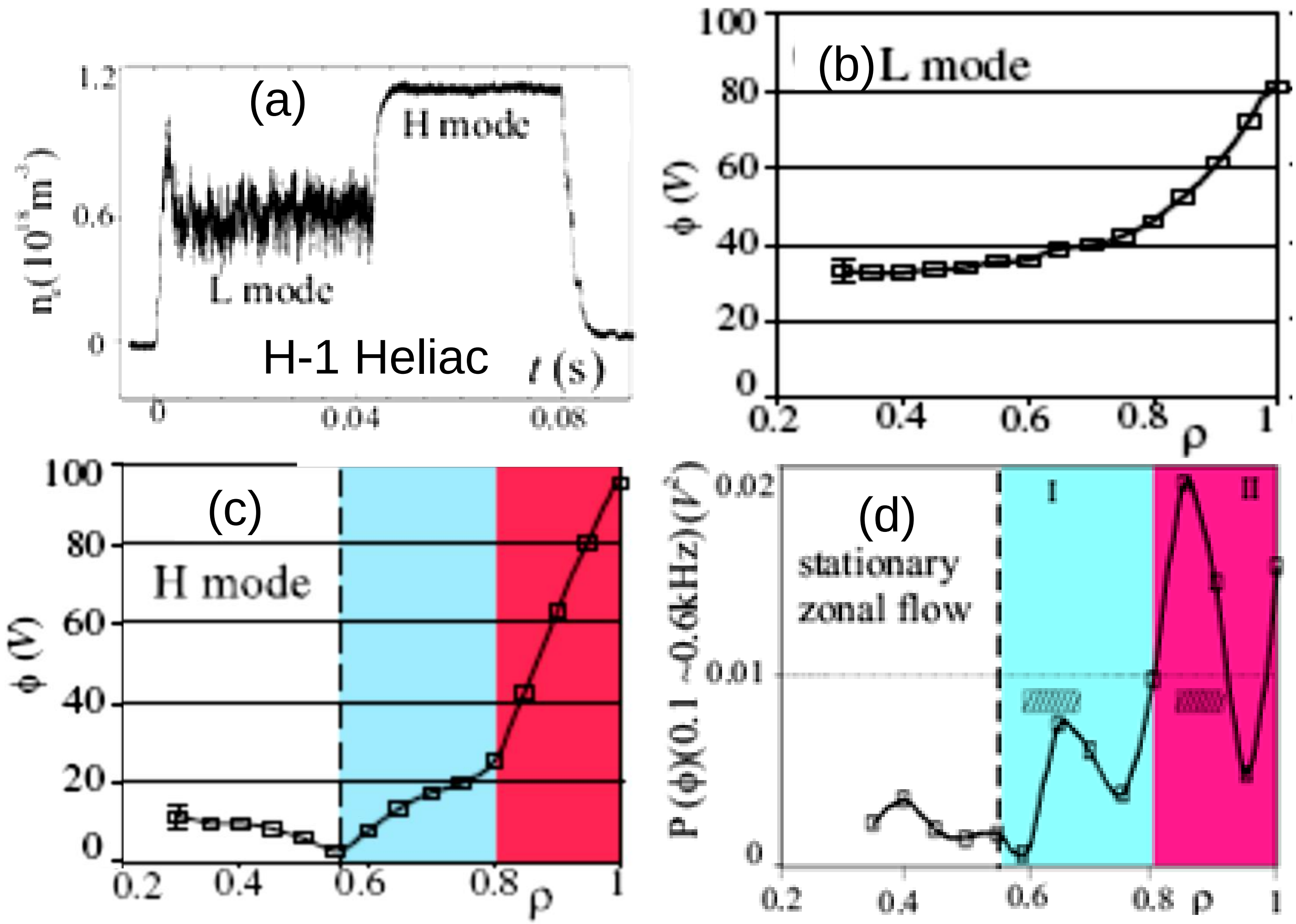

Spectral power density of zonal flows

H. Xia et al., Phys. Rev. Letters

Conjecture: E_r-field caused by zonal flows

Paradigma for the L-H Transition at “linear conditions” H-1

Spectra of potential fluctuations in L and H-modes.

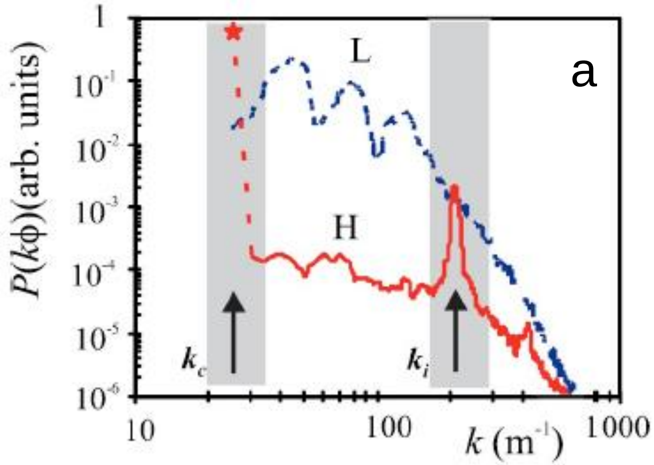

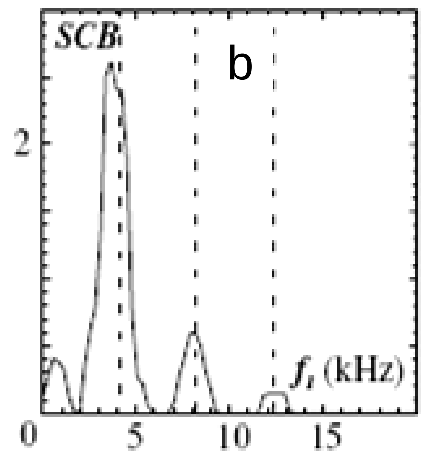

Summed Cross-bi-Coherence

Measure of 3-wave coupling

Non-linear energy transfer function indicating 3-wave coupling

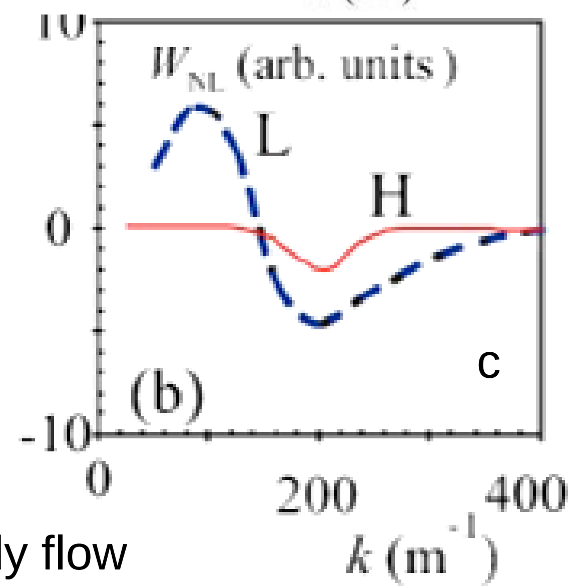

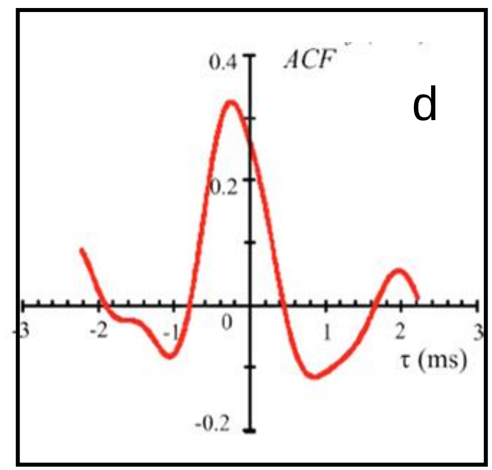

L-mode: spectral transfer From higher to lower k

H-mode: transfer to steady flow

Amplitude correlation function between two bands
– one at injection k, k_i,
the other in the k-range of large poloidal structures.

M. G. Shats et al., Phys. Rev. Letters
M. G. Shats et al., Phys. Review E

Summary of the H-1 results

- Drift-wave turbulence injected at k_i = 200 m^{-1} (p´; linear instability range)
- Energy cascades to smaller and larger k via 3-wave coupling
- The plasma boundary limits the largest possible scale
- Spectral energy is transferred into coherent modes: time varying zonal flows
- Spectral energy accumulates at $k = k_c \rightarrow 0$; turbulence „condenses“
- In the experiment, large m=0 (+side band) structures appear: mean ZF, E_r-shear

- Simultaneously, the broad-band turbulence disappears: H-transition
- The kinetic energy of the resulting flow agrees with the pot. energy of the turbulence field within 20%
- The injection DW at k_i remains, even intensifies (p´)
- Spectral energy transfer between k_i and k_c maintains flow
- This non-local transfer process (between well separated spectral ranges) prevents turbulence: confinement increases

Related Observations on W7-AS

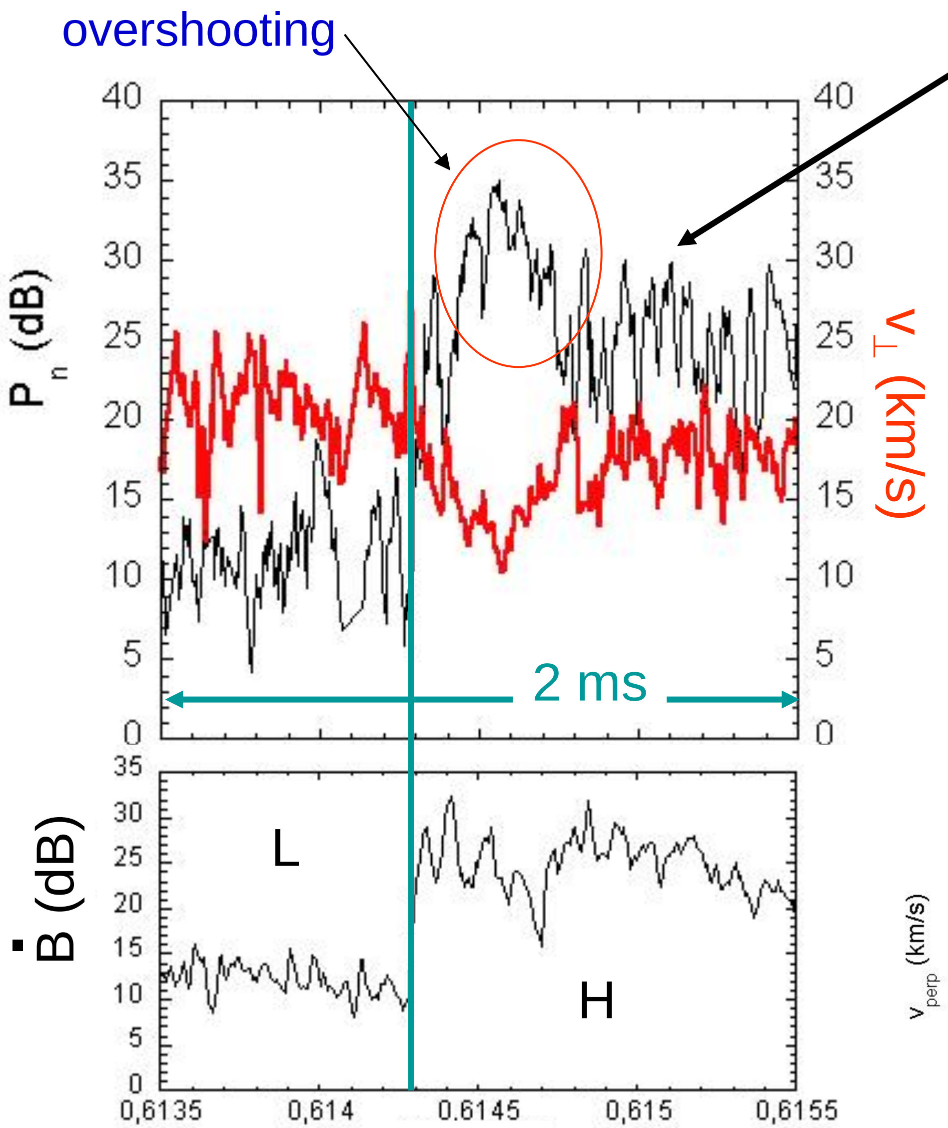

Fluctuations at 11 kHz
(corresponds to GAM frequency)

Phase before transition:
P_n and $v_\perp$ anticorrelated
P_n leads $v_\perp$ by 10 μs

Phase after transition:
P_n and $v_\perp$ are correlated

Transition in downswing of $v_\perp$
P_n increases and continues

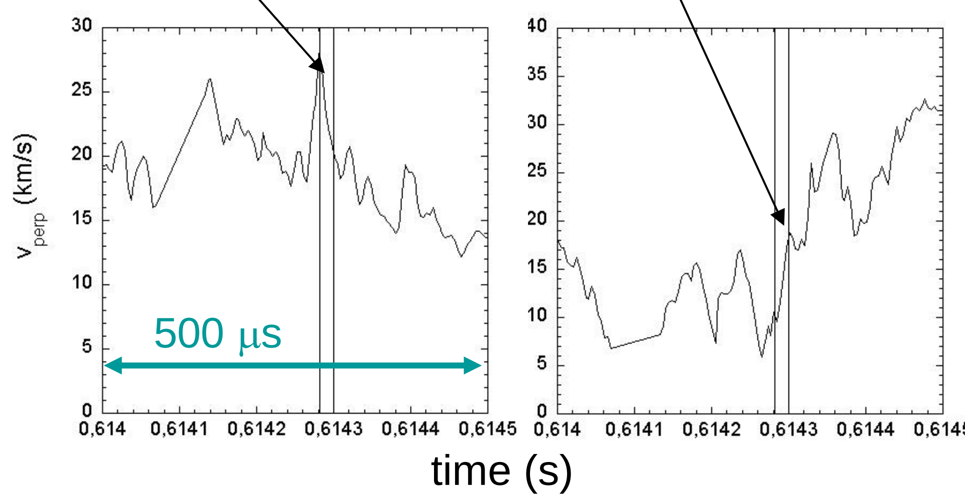

7 Achievements in the H-mode

The 16.1 MW DT discharge of JET

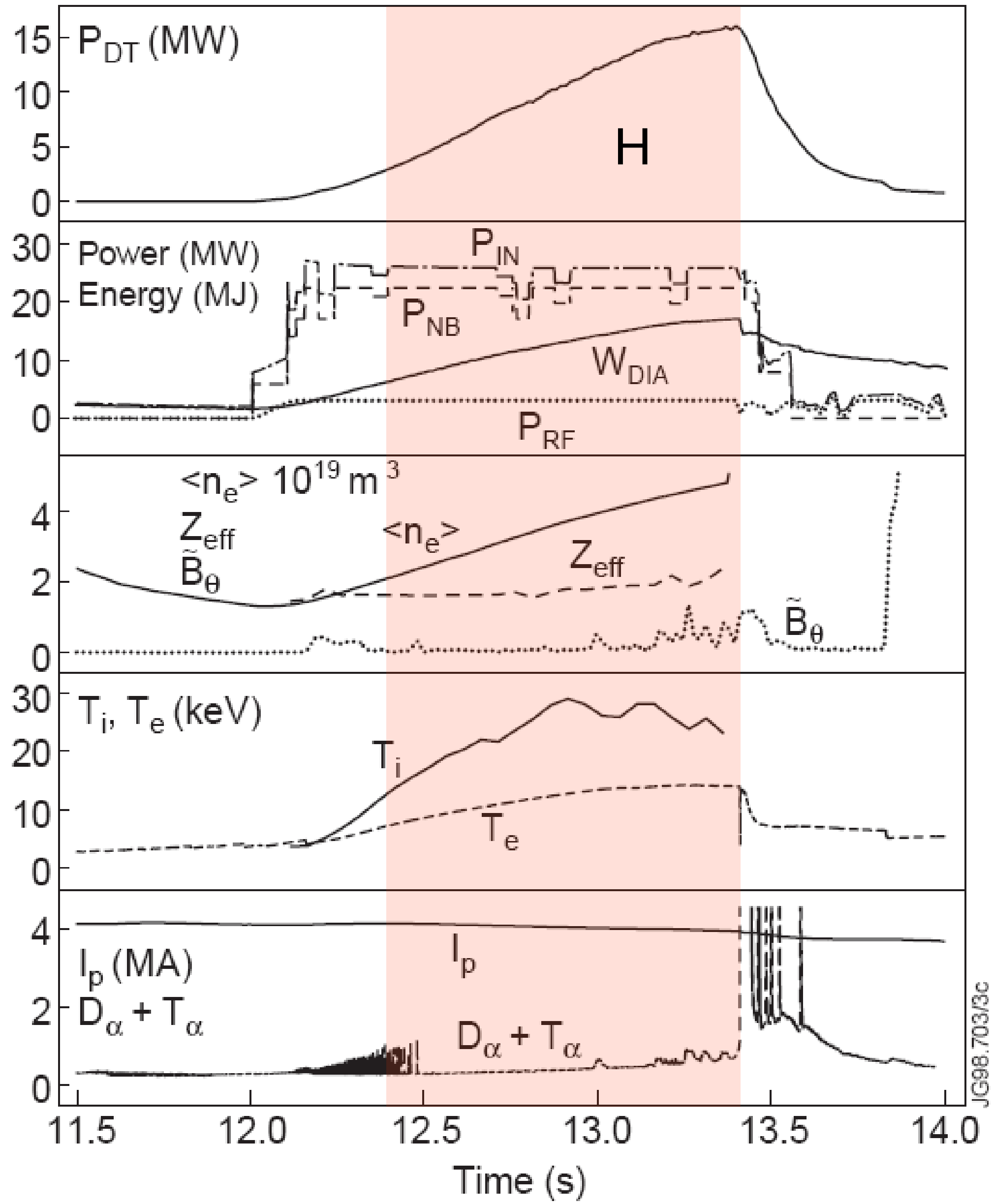

High-performance discharges: Tokamak

Ip (x10) MA
P_{NBI} MW

Magn. perturbation
n=3, n=2, n=1

D_{α}, upper divertor

β_N
$4l_i$

q_{min}
q(0)

n_e
Z_{eff}

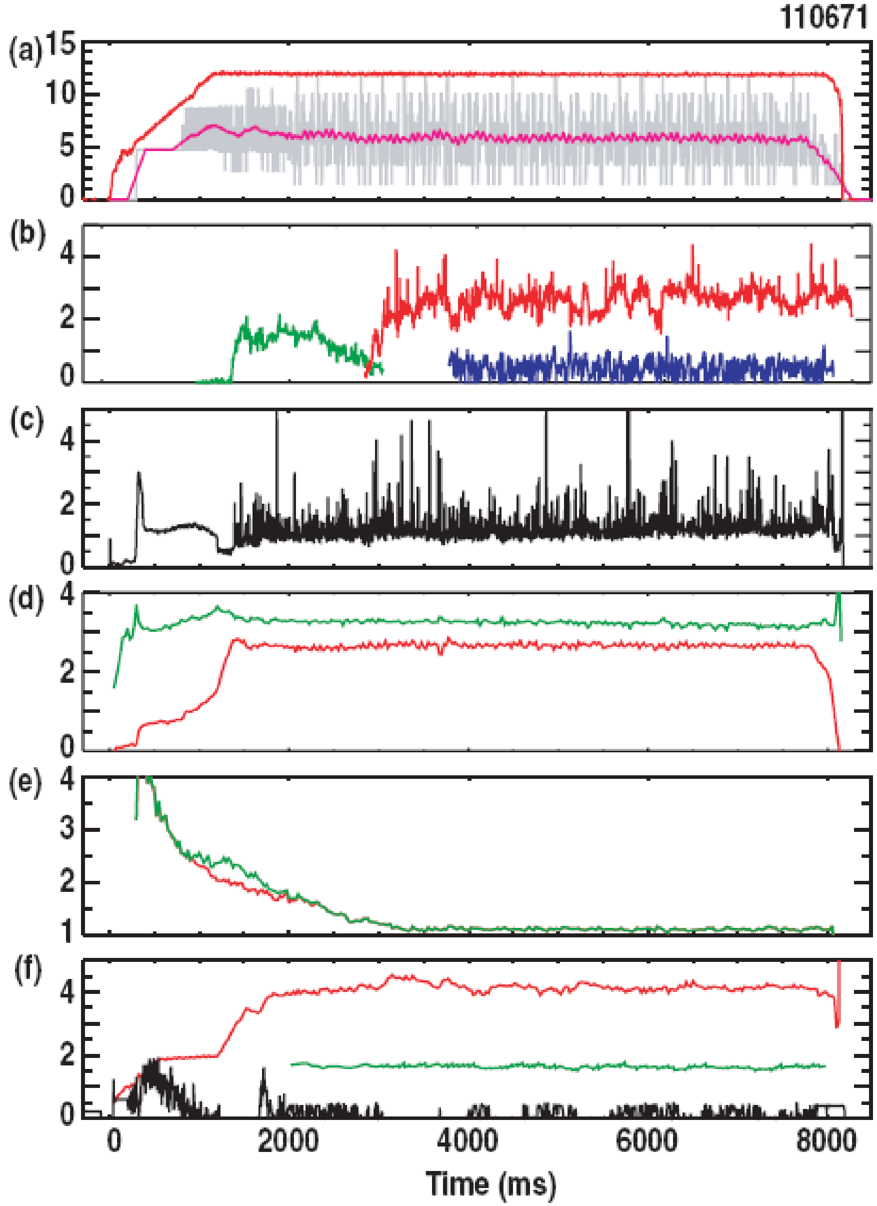

DIII-D*
*Prize at last IAEA

$n_e = 0.4\ 10^{20}\ m^{-3}$
$P_{NBIabs} = 4.8$ MW.

$\beta \sim 3\%$
$\beta_N = 2.7$
$H_{89} = 2.6$
$n_e/n_{eGW} = 0.4$

Mapped to ITER
Q=10

Steady-state
$\Delta t \sim 36\ \tau_E$

Long-pulse HDH discharge of W7-AS

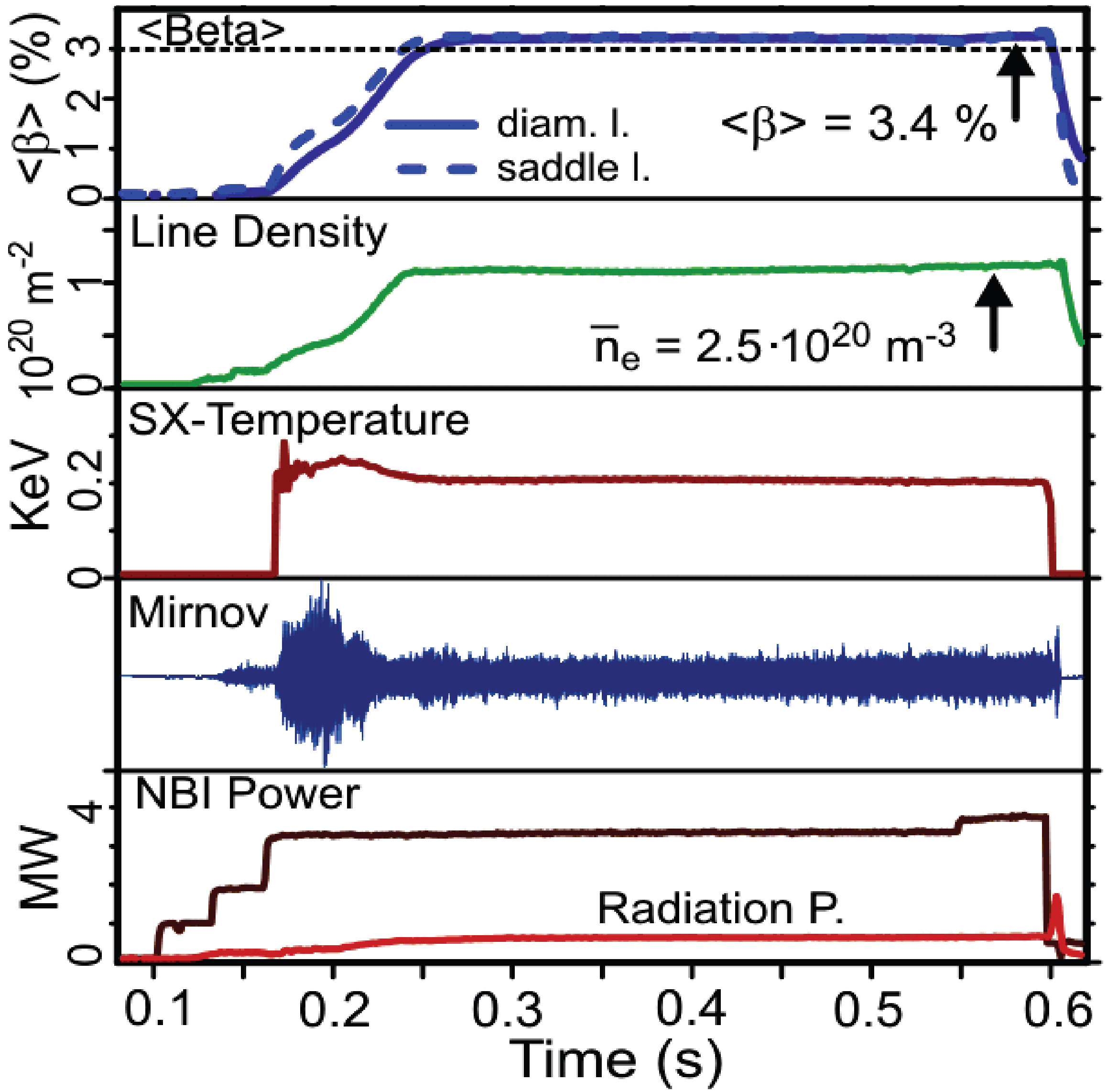

HDH regime

$B = 0.9$ T
$n_e = 2.5\ 10^{20}\ m^{-3}$
$P_{NBIabs} = 2.5$ MW

$\beta = 3.4\%$
$\beta_N \sim 9.3$
$H_{ISS95} = 1.4$
$n_e/n_{eGW} = 2.5$
$\tau_I/\tau_E \sim 2$
$\Delta t \sim 36\ \tau_E$

H-mode as confinement basis for ITER

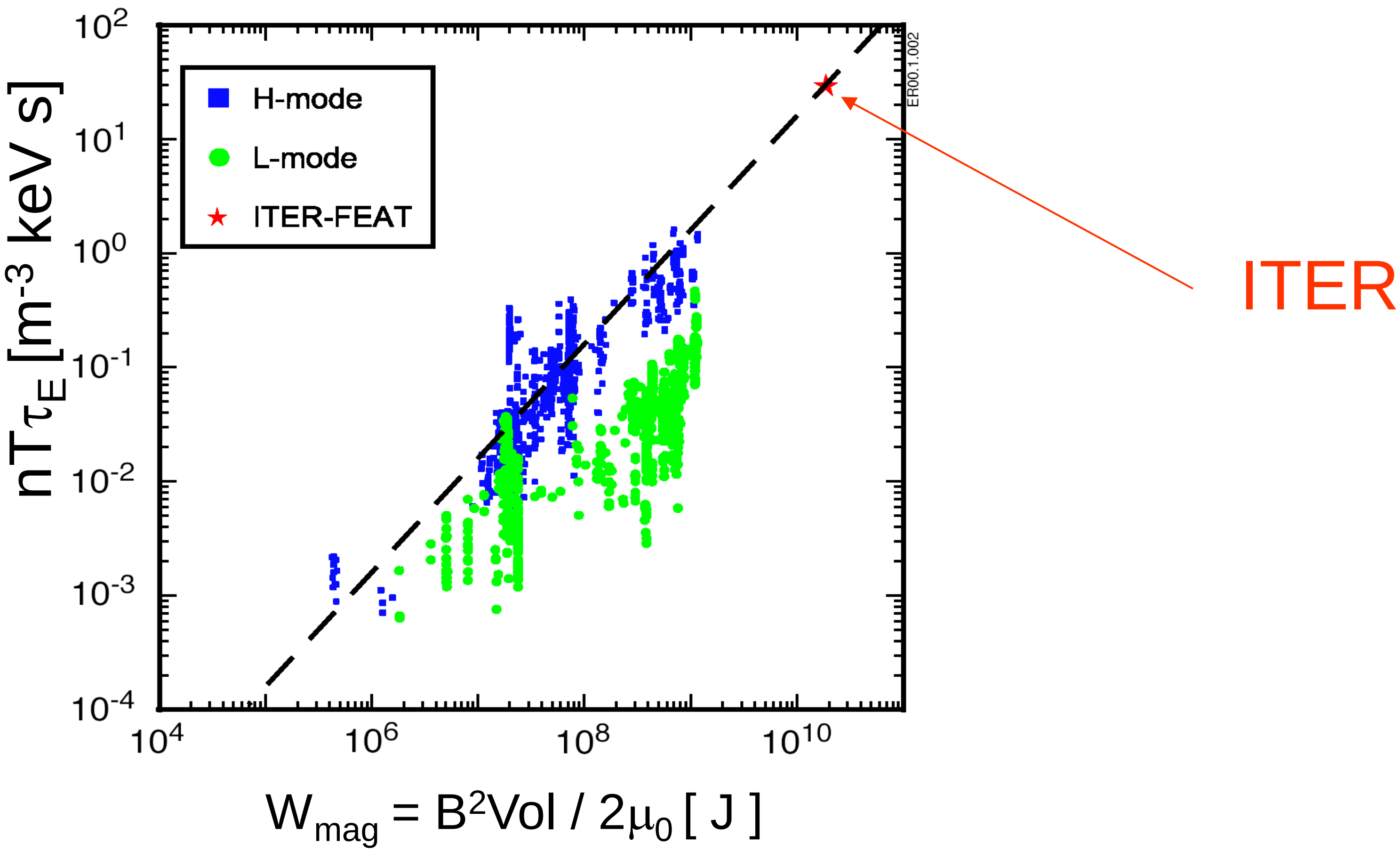

Cost scaling: \$ ~ $H^{-1.3}$ *

H-mode ITER: 5 Bill €

Equivalent L-mode ITER: 12.3 Bill €

* S-I Itoh, K Itoh, and Fukuyama, Fusion Engineering and Design

8 ELMs

Edge localised modes

repetitive destruction of edge transport barrier

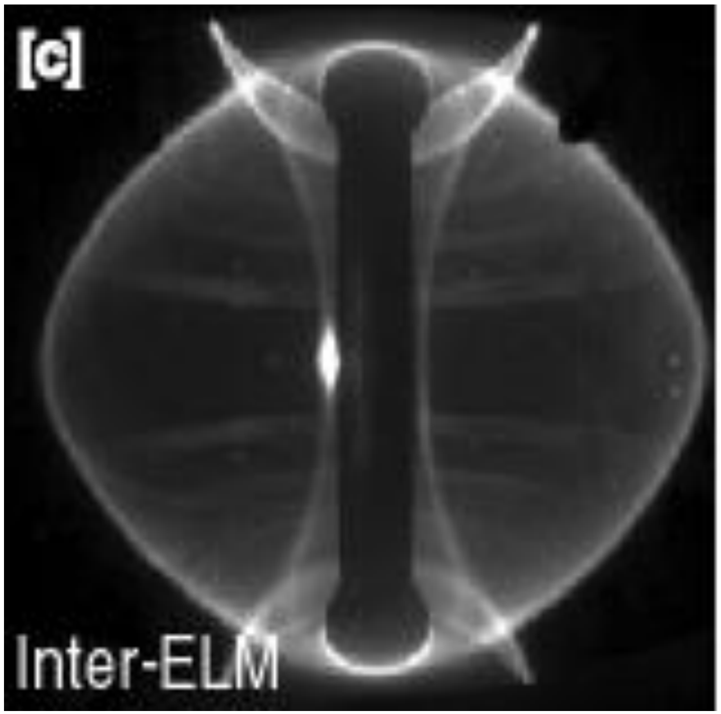

Between ELMs

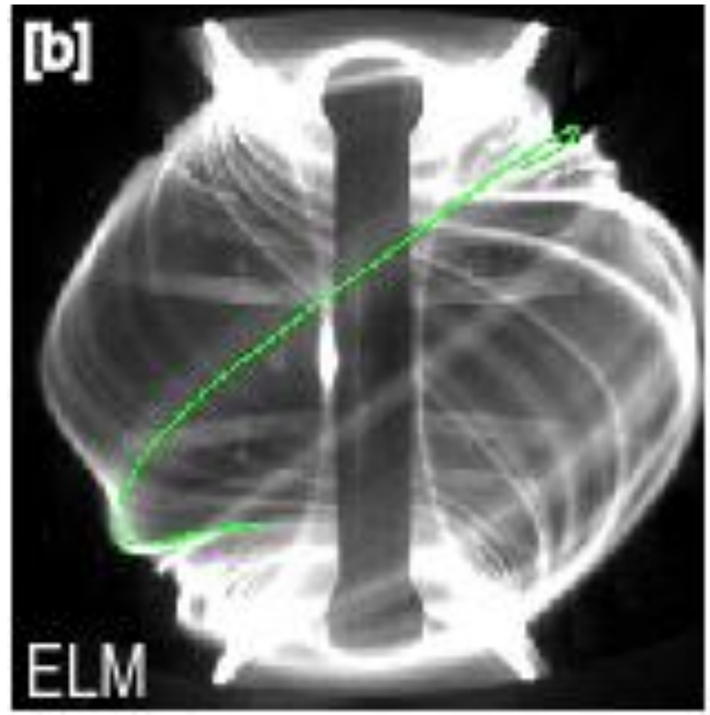

ELM

N. Ben Ayed, MAST

ELMs

Edge localised modes

repetitive destruction of edge transport barrier

MHD event or limit-cycle? Often there is an MHD precursor

ELMs can be singular and large

or they can be frequent and erratic

Different types of ELM are discriminated

Typ-I ELMs: large, more ideal MHD instabilities

Typ-III ELMs: small, frequent, more resistive MHD

driven by edge pressure gradient and/or edge bootstrap current

BUT: Bootstrap current in stellarator edge is low

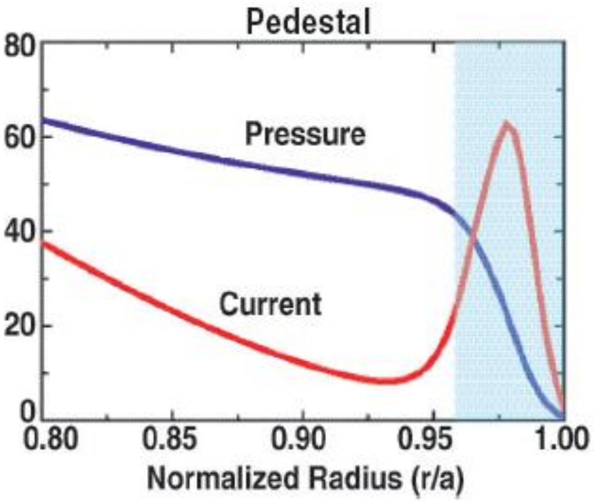

Edge pedestal DIIID (R. Stambaugh)

ELMs and plasma-wall interaction

Repetitive destruction of barrier

JET

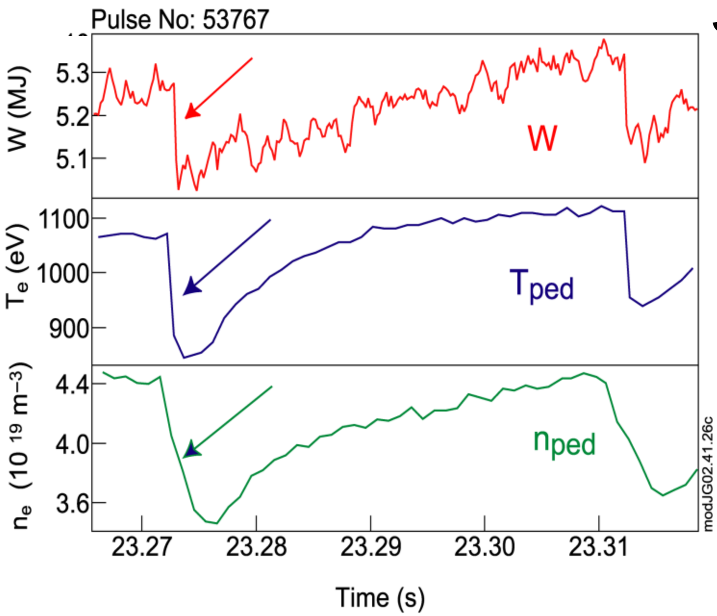

A. Loarte, PPCF 2002

Power loading in ITER

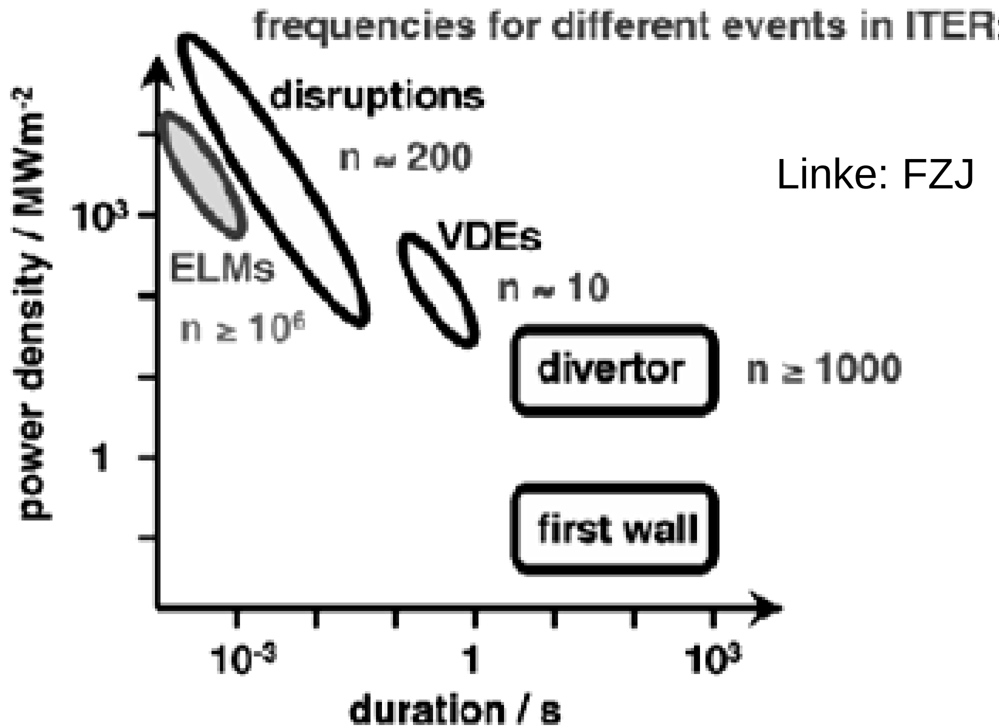

Linke: FZJ

JET : ΔW_{ELM} ~ 1 MJ and τ_{ELM} ~ 100 μs → P_{ELM}^{PFCs} ~ 10 GW ($P_{steady\text{-}state}$ = 10 MW)

ITER : ΔW_{ELM} ~ 20 MJ; f_{ELM} ~ Hz

E_{div} > 2.5 MJm^{-2} & q_{div} > 5 - 10 GWm^{-2} in ~ 250-500 μs → Δ_{ELM} > 10 μm

ELM mitigation by partial edge ergodisation

DIIID: use of perturbation coils

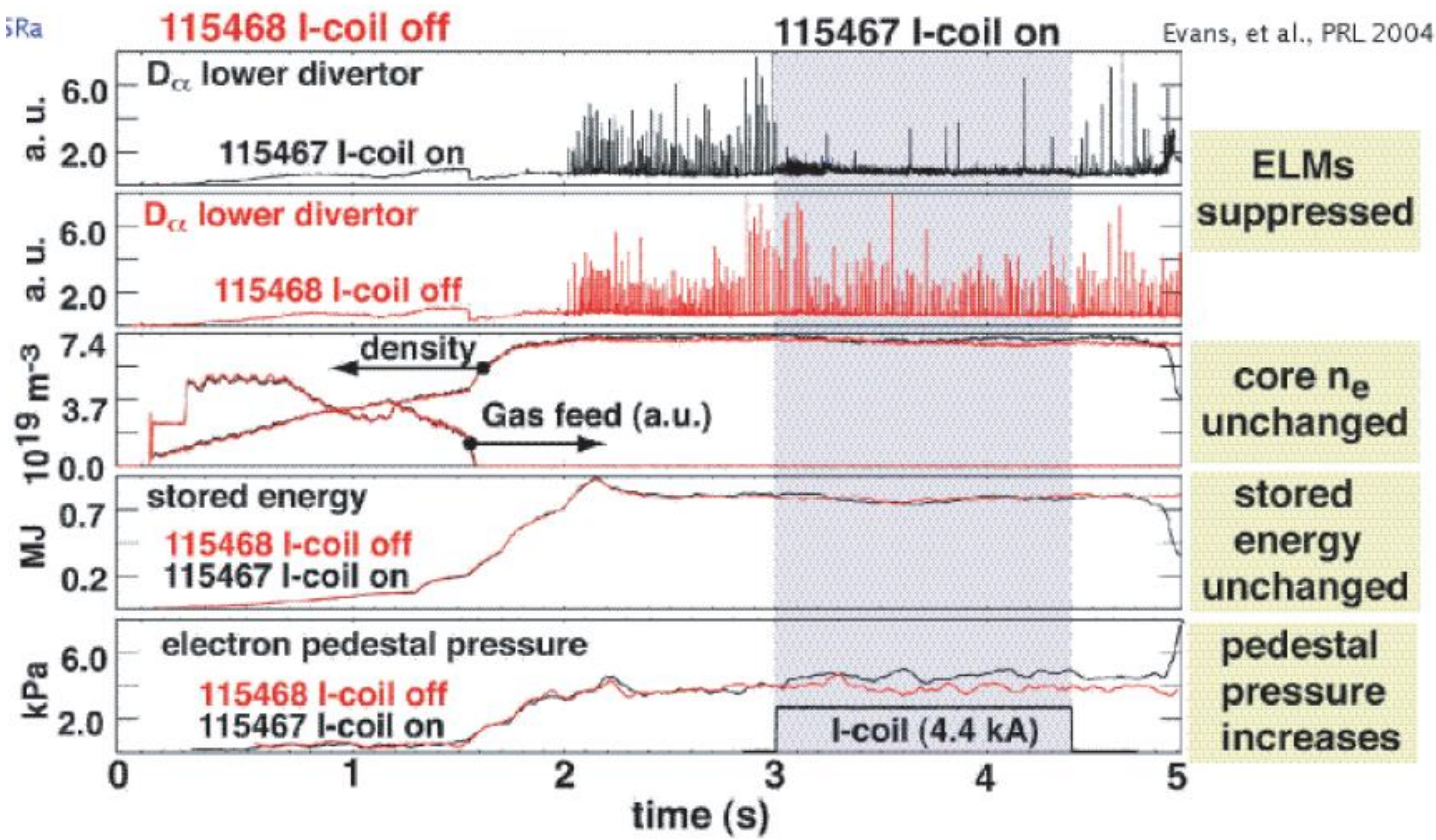

Alternative: slow pellet injection

9 Summary

The plasma self-organises in the H-mode such
 that the turbulence is lower at larger driving forces
 and that the ignition conditions are approached

The H-mode has inspired theory to develop a better understanding of turbulent transport

The situation is involved however:

- There are many practical knobs to realise and develop the H-mode
- An understanding might have to involve the
  - power balance
  - the toroidal momentum balance
  - the poloidal momentum balance
  - The transformation of turbulent energy into flow
  - the SOL flow and viscous momentum transfer
- The many practical knobs may indicate that several mechanisms are involved

The H-mode is a contribution to the physics of highly non-linear hydro-dynamic systems

Summary

There is no complete understanding of the H-transition

- ion-loss concept
- high poloidal mach numbers
- the role of parallel viscosity and the damping of zonal flows
- the interface with the SOL
- the actual trigger condition to the H-mode
- the self-consistent E_r-field development and turbulence quench
- the P_{th}-scaling
- the ion-grad B effect
- modelling of a complete cycle: L=>H and back H=>L

More has to be understood about ELMs and ELM-mitigation